Icelandic
Meteorological Office

Veðurstofa
Íslands

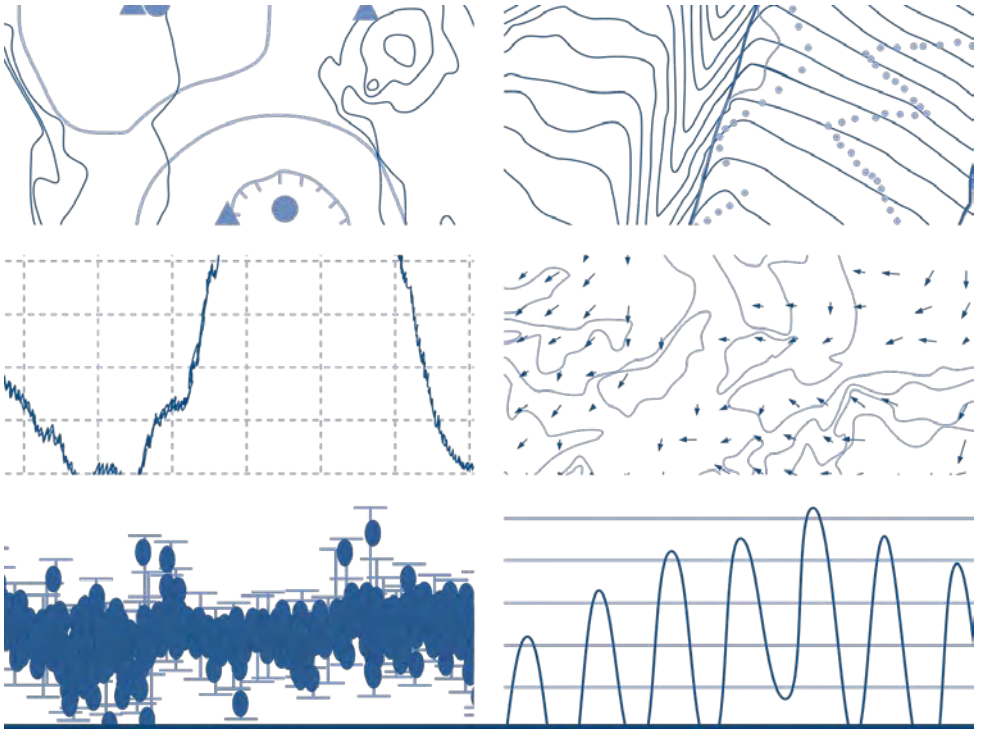

# Surface Wind and Air Temperature over Iceland based on Station Records and ECMWF Operational Analyses

Nikolai Nawri
Halldór Björnsson
Guðrún Nína Petersen
Kristján Jónasson

**Report**

VÍ 2012-008

Icelandic
Meteorological Office

Veðurstofa Íslands

# Surface Wind and Air Temperature over Iceland based on Station Records and ECMWF Operational Analyses

Nikolai Nawri, Icelandic Met Office
Halldór Björnsson, Icelandic Met Office
Guðrún Nína Petersen, Icelandic Met Office
Kristján Jónasson, University of Iceland

**Report**

Veðurstofa Íslands
Bústaðavegur 7–9
150 Reykjavík

+354 522 60 00
vedur@vedur.is

VÍ 2012-008
ISSN 1670-8261

**Keypage**

Veðurstofa Íslands

| Report no.: | Date: | ISSN: | Public ☒ Restricted ☐ |
|---|---|---|---|
| VÍ 2012-008 | September 2012 | 1670-8261 | Provision: |

| | |
|---|---|
| **Report title / including subtitle**<br>Surface Wind and Air Temperature over Iceland based on Station Records and ECMWF Operational Analyses | **No. of copies:** 20<br>**Pages:** 55 |
| | **Managing director:**<br>Jórunn Harðardóttir |
| **Authors:**<br>Nikolai Nawri<br>Halldór Björnsson<br>Guðrún Nína Petersen<br>Kristján Jónasson | **Project manager:**<br>Halldór Björnsson |
| | **Project number:**<br>5813-0-0004 |
| **Project phase:** | **Case number:**<br>2012-333 |

**Report contracted for:**
IceWind Project

**Prepared in cooperation with:**


**Summary:**
In this study, seasonal averages and temporal variability on different time-scales of surface wind and air temperature over Iceland are analysed. For weak winds, the influence of temperature gradients is clearly noticeable at nearly all locations. Especially during winter, prevailing surface winds flow from low to high temperatures, downslope in the interior of the island, and off-shore along the coast. In summer, land-sea temperature gradients result in prevailing on-shore winds in most places. For intermediate to strong surface winds in both seasons, easterly and south-easterly directions prevail near the coast in the western part of the island, where large scale geostrophic winds combine with local temperature gradients. Temporal variability of wind speed generally decreases from the centre of the island outwards.



**Keywords:**
Surface wind speed, surface air temperature, station data, ECMWF operational analyses, seasonal averages, temporal variability, Iceland


**Managing director's signature:**

**Project manager's signature:**

**Reviewed by:**

# Contents

**1 Introduction** **7**

**2 Data** **8**

**3 Geography** **10**

**4 Methodology** **18**
4.1 Selection of Local Values from Analysis Fields . . . . . 18
4.2 Stereographic Projection of Wind Vectors . . . . . 23

**5 Seasonal Averages** **24**
5.1 Surface Wind . . . . . 24
5.2 Surface Air Temperature . . . . . 29

**6 Temporal Variability** **33**
6.1 The Seasonal Cycle . . . . . 33
6.2 Surface Wind . . . . . 35
6.3 Surface Air Temperature . . . . . 39

**7 Summary** **45**

**A Surface Weather Stations** **48**

# List of Figures


1 Annual surface wind speed data availability . . . . . 8
2 Terrain elevation in operational analyses and digital terrain models . . . . . 9
3 Topography and locations of surface weather stations in northwest Iceland . . . . . 11
4 Topography and locations of surface weather stations in northern Iceland . . . . . 12
5 Topography and locations of surface weather stations in eastern Iceland . . . . . 13
6 Topography and locations of surface weather stations in southern Iceland . . . . . 14
7 Topography and locations of surface weather stations in southwest Iceland . . . . . 15
8 Terrain statistics within 1 km around weather station locations . . . . . 16
9 Terrain statistics within 30 km around weather station locations . . . . . 17
10 Seasonal mean sea level pressure based on operational analyses . . . . . 19
11 Seasonal surface wind speed based on operational analyses . . . . . 20
12 Seasonal surface air temperature based on operational analyses . . . . . 21
13 Comparison of different interpolation methods . . . . . 22
14 Average surface wind speed based on measurements and operational analyses . . . 25
15 Average surface wind vectors for low surface wind speeds . . . . . 26
16 Average surface wind vectors for intermediate to high surface wind speeds . . . . . 28
17 Average surface air temperature based on measurements and operational analyses . 30
18 Seasonal observational temperature, for on-shore or off-shore winds . . . . . 31
19 Seasonal analysed surface air temperature, for on-shore or off-shore surface winds . 32
20 Seasonal cycle of surface air temperature for different station elevations . . . . . 35
21 Seasonal cycle of surface air temperature for different regions . . . . . 36
22 Seasonal cycle of surface wind speed for different station elevations . . . . . 37
23 Seasonal cycle of surface wind speed for different regions . . . . . 38
24 Temporal variability on seasonal and sub-monthly time-scales of surface wind speed 40
25 Root mean square tendency of surface wind direction as a function of wind speed . 41
26 Root mean square tendency of surface wind direction for low surface wind speeds . 42
27 Tendency of surface wind direction for intermediate to high surface wind speeds . . 43
28 Temporal variability of surface air temperature on different time-scales . . . . . 44

# 1 Introduction

In this study, seasonal averages and temporal variability on different time-scales of surface wind and air temperature over Iceland are analysed. It is part of research conducted by the University of Iceland (Háskóli Íslands; UI) and the Icelandic Meteorological Office (Veðurstofa Íslands; IMO), in the context of the project "Improved Forecast of Wind, Waves and Icing" (IceWind), funded primarily by the Norwegian Top-Level Research Initiative (Toppforskningsinitiativet; TFI), in collaboration with national and private organisations in other Nordic countries. More specifically, the work done at UI and IMO is part of IceWind Work Package 2, the goal of which is the development of a wind atlas for Iceland, the identification of suitable wind farm sites, as well as carrying out technical and market integration studies.

The primary data source for the wind atlas are mesoscale simulations, obtained with the Weather Research and Forecasting (WRF) Model (Skamarock et al., 2008). To be able to evaluate the accuracy of the model data, the goal of this study is to provide an observational basis for the recent prevailing surface wind and air temperature conditions over Iceland. Although the main focus of IceWind Work Package 2 is on winds, surface air temperature is included in the analysis due to its close connection to atmospheric motion, and its importance for icing. The results discussed here are based on station records, as well as operational analyses produced by the European Centre for Medium-Range Weather Forecasts (ECMWF), through four-dimensional variational data assimilation, combining different types of observational data with *a priori* fields from short-term predictions of the global meteorological model (Courtier, 1997; Andersson and Thépaut, 2008).

In this first of a series of reports, the climatological conditions at weather station locations are analysed. Wind data are corrected for differences in anemometer heights. Otherwise, no attempt is made to account for terrain effects, or sheltering and speed-up from local obstacles. Operational analyses are included here for comparison, as they only contain large-scale effects, and no impact from local obstructions. Gridded terrain models based on station data, covering all of Iceland and, in simplified form, taking into account terrain elevation and sheltering, are discussed in Nawri et al. (2012a). A comparison of local station data and terrain models for surface wind with WRF model simulations is given in Nawri et al. (2012b), and a statistical correction of WRF model data based on these comparisons is discussed in Nawri et al. (2012c).

# 2 Data

Quality controlled hourly surface measurements of wind speed and direction, as well as air temperature, were obtained from the Icelandic Meteorological Office. Winds are measured at different heights $h$ above ground level (AGL), varying between 4.0 and 18.3 m. These differences are taken into account following WMO guidelines (WMO, 2008), whereby wind speeds are projected to 10 mAGL by

$$S(10\text{m}) = S(h)\,\frac{\ln(10/z_0)}{\ln(h/z_0)}\,, \tag{1}$$

where for Iceland the surface roughness length $z_0$ over land is approximately 3 cm (WMO, 2008). Surface air temperature is measured at 2 mAGL. The names, ID numbers, and coordinates of all stations from which data was used are given in Tables 1 and 2, in alphabetical and numerical order, respectively.

For any given variable, only those locations are considered, for which station records have at least 75% valid data within any specific period under consideration. As a result of these selection criteria, the stations shown in different figures may vary, depending on the variable and the season. The lower limit of data availability is introduced to avoid biases in inter-station comparisons, which may arise due to uneven missing data within a certain time period at some locations.

Thereby a compromise needs to be made between temporal coverage at individual locations, and spatial coverage, determined by the number of stations with sufficient temporal data availability. As seen in Figure 1, over the last decade there has been a steady increase in the number of stations with 75% of valid hourly surface wind speed data within each year.

With a total of 145 stations with some wind data at any time within 2000-10, from 2006 onwards, 75% of all stations have a temporal coverage for surface wind speed of 75%. WRF model simulations, which are used in related analyses, are available from 1 Sep 1994 until 2 Nov 2009. Since the emphasis of IceWind is on establishing the current and recent past surface wind field over Ice-

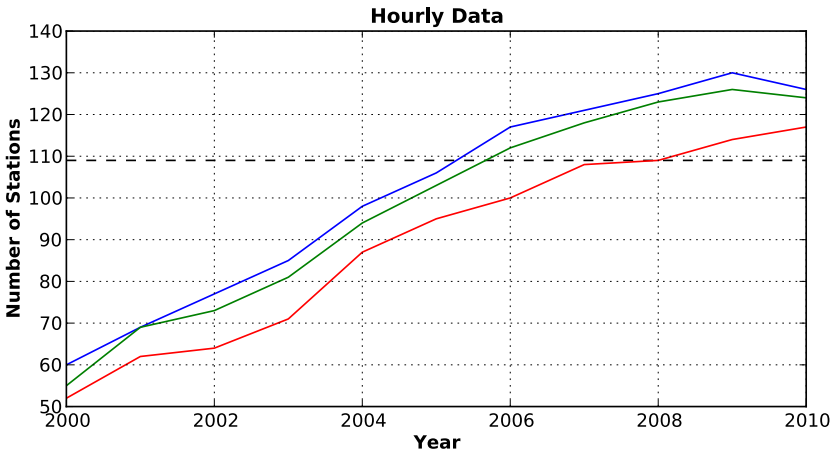


*Figure 1. Number of stations with at least 50% (blue lines), 75% (green lines), and 95% (red lines) of valid surface wind speed data within a given year. The dashed line at 109 represents 75% of the total number of stations (145).*

land and its spatial and temporal variability, rather than its longterm climatological conditions, the study presented here is limited to the 4-year period from 1 Nov 2005 until 31 Oct 2009, which is covered by the WRF simulations, and provides the best balance between temporal and spatial coverage.

Also used in this study are 6-hourly operational surface analyses for air pressure, temperature, wind, and sea surface temperature from ECMWF, valid at 00, 06, 12, and 18 UTC (which is local time in Iceland throughout the year). For the purpose of comparisons with operational analyses, station data is reduced to the same 6-hourly time-step. The highest available resolution of analysis fields is 0.125 degrees in longitude and latitude. A similar physical grid-spacing in meridional and zonal direction over Iceland results with twice the angular grid-spacing in longitude. For time-series derived from the operational analyses for specific station locations, a comparison is made between fields with two different spatial resolutions: low-resolution fields with an angular grid-spacing of 0.50 degrees in longitude, and 0.25 degrees in latitude; and high-resolution fields with an angular grid-spacing of 0.250 degrees in longitude, and 0.125 degrees in latitude. The physical grid-spacing is then 27.8 and 13.9 km in latitude, respectively. In longitude, along 65°N, the physical grid-spacing is 23.5 and 11.7 km, respectively. The model terrain at both resolutions, derived from the geopotential at the surface, is shown in Figure 2.

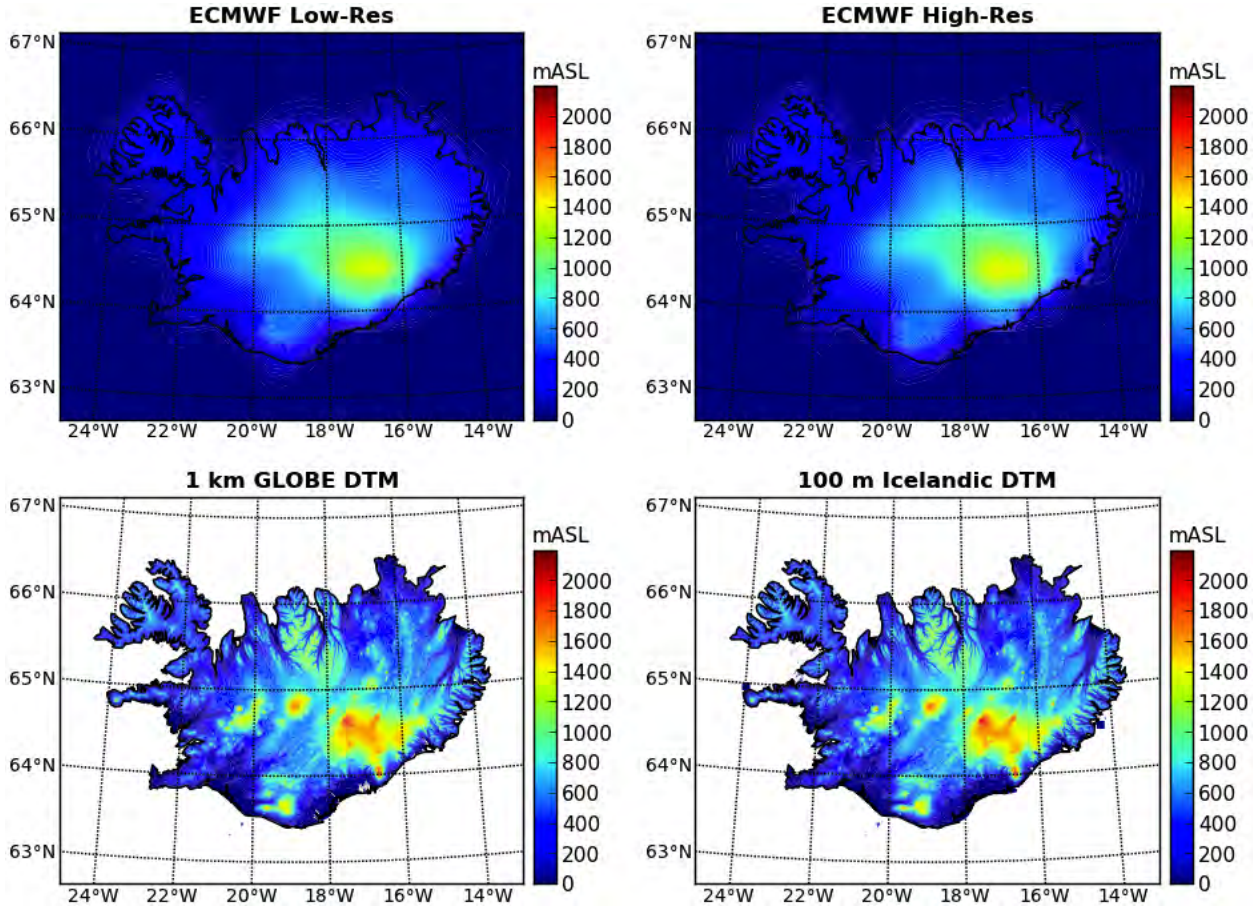


*Figure 2. Terrain elevation as represented in operational analyses, as well as based on the GLOBE and Icelandic digital terrain models (DTMs, see Section 2).*

To relate the spatial variability of surface variables to terrain characteristics, a digital terrain model (DTM) at a $100 \times 100$ m resolution was used (see Figure 2). This DTM was produced in 2004 by the Icelandic Meteorological Office, the National Land Survey of Iceland (Landmælingar Íslands), the Science Institute of the University of Iceland (Raunvísindastofnun Háskólans), and the National Energy Authority (Orkustofnun).

For plotting purposes, lower-resolution digital elevation data from the Global Land One-km Base Elevation Project (GLOBE), produced by the National Geophysical Data Center of the U. S. National Oceanic and Atmospheric Administration, is used (see Figure 2). It has a homogeneous 30-arcsecond angular resolution.

# 3 Geography

The locations considered in this study, within the context of the GLOBE topography, are shown in Figures 3 to 7. In regions with a high density of stations, some numbers are omitted for clarity. Station locations are then indicated by black dots only.

There are large differences in the density of stations across Iceland, with the highest number of stations on Reykjanes in the southwest, around Egilsstaðir in the east, and around Akureyri in the north. All stations included in this study are located below 900 m above mean sea level (mASL), with 88 of the 145 stations (61%) located below 100 mASL. There are therefore no stations on any of the glaciers. Additionally, no data is available for a large region with terrain mostly below 1000 mASL, extending northward from Vatnajökull and eastward from Mývatn to the coast. The average shortest horizontal distance[1] between two stations is 15 km, with a maximum of 50 km.

Terrain statistics within 1 km around each station location, derived from the 100-m-resolution DTM, are shown in Figure 8. Sheltering is defined as the difference between the maximum terrain elevation within the 1-km radius, and the local elevation. Terrain slope is defined as the magnitude of the local elevation gradient. Regional averages of terrain slope are distance weighted with exponential function $\exp(-a\,r)$, where $r$ is the distance from the station location, and $a = \log(2)/r_h$, with half-width $r_h = 1$ km. Local elevation generally increases towards the interior of the island, but a few elevated sites are within 30 km of the coast. Sheltering is largest in the Westfjords, where weather stations are situated at low elevations within complex and high terrain. Intermediate sheltering is found in the east. Within the short distance of 1 km, characterising the immediate station surroundings, elevation standard deviation and average slope show a similar spatial distribution as sheltering. Terrain statistics within 30 km around each station are shown in Figure 9. Here, elevation difference is defined as the difference between local terrain elevation and average elevation, distance weighted as above, but with half-width $r_h = 30$ km. On this scale, resolved at least by high-resolution operational analyses, the regional pattern of ruggedness becomes more apparent, with some exposed stations primarily in the southwest, and sheltered stations primarily in the Westfjords, in the north, and east.

[1] All horizontal distances in this study are calculated along great circles on a spherical Earth at mean sea level.

Land surface area above a certain altitude, and therefore surface friction, decreases with altitude, accompanied by a reduction in surface roughness, as tall vegetation and built-up areas become increasingly sparse. Even without stronger forcing, this generally leads to an increase in surface wind speed with terrain elevation. At a given elevation, terrain surface area per unit horizontal area, and therefore surface friction, increases with ruggedness, such as measured by terrain slope. This contributes to a reduction of surface wind speed over complex terrain. Additionally, under stable flow conditions, blocking locally reduces wind speed, whereas channelling and flow over low hills increases wind speed. The combined effects of elevated terrain on surface winds, even qualitatively, is therefore difficult to predict.

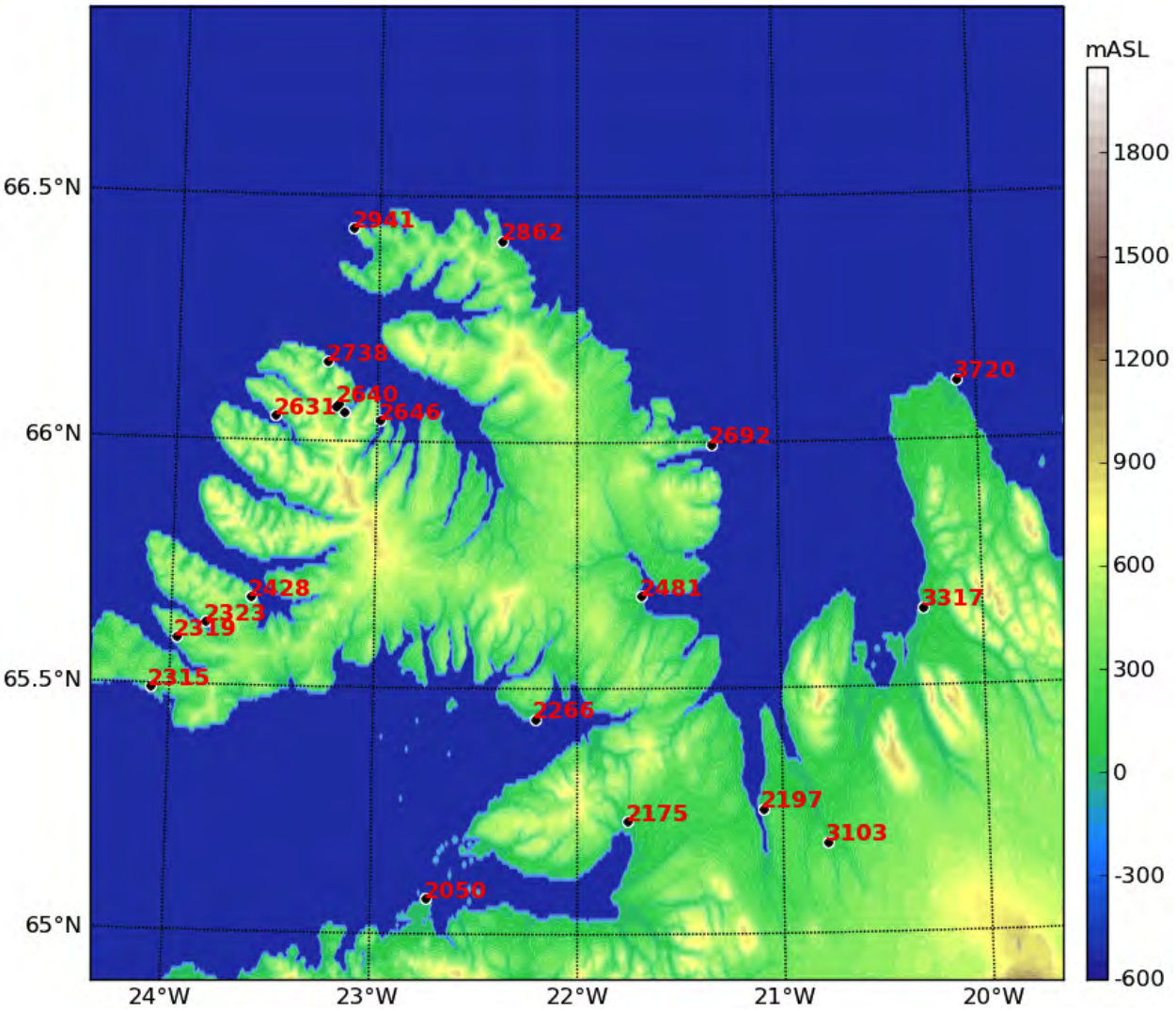


*Figure 3. Topography (based on the GLOBE digital terrain model) and locations of surface weather stations in northwest Iceland.*

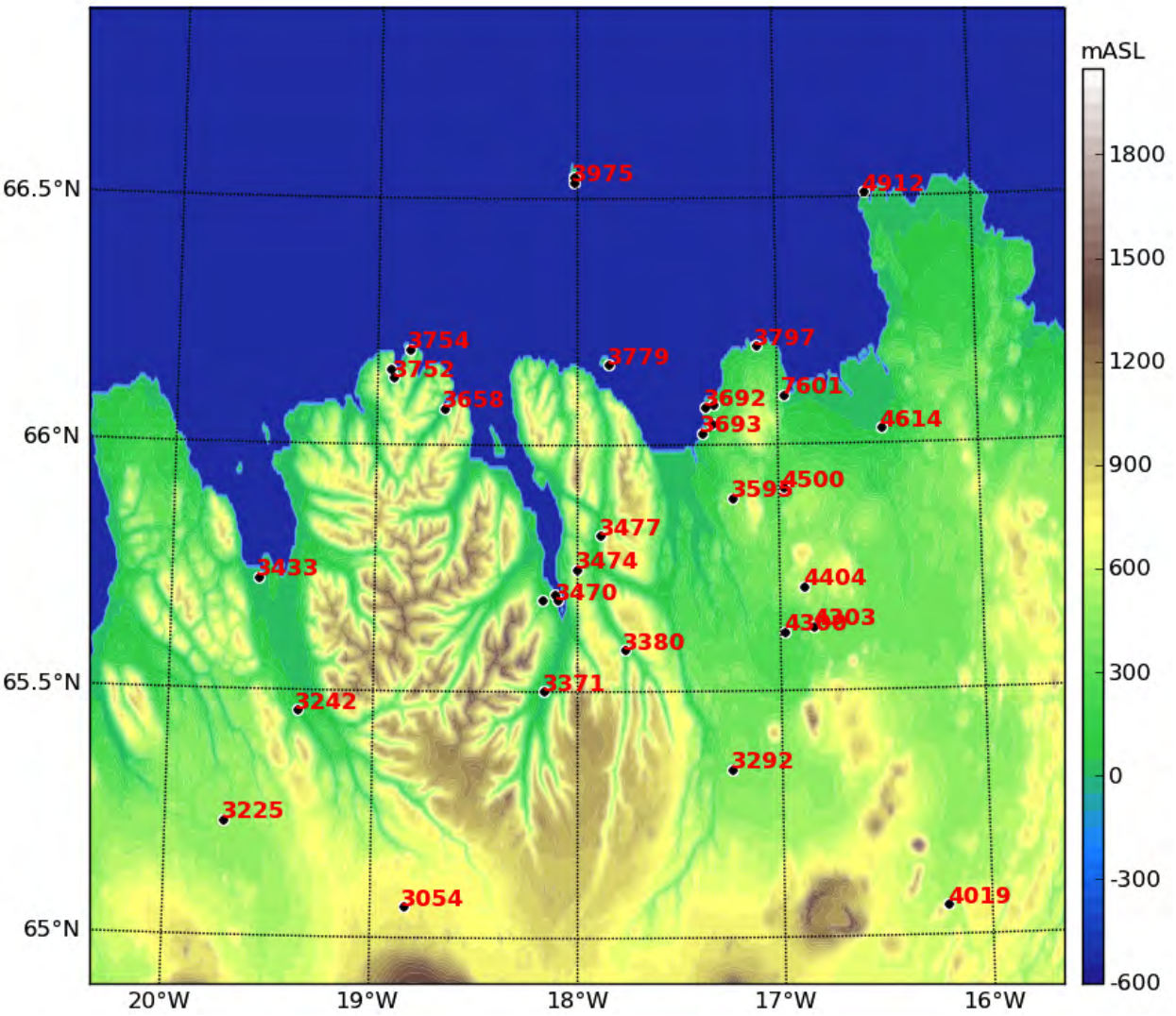


*Figure 4. Topography (based on the GLOBE digital terrain model) and locations of surface weather stations in northern Iceland.*

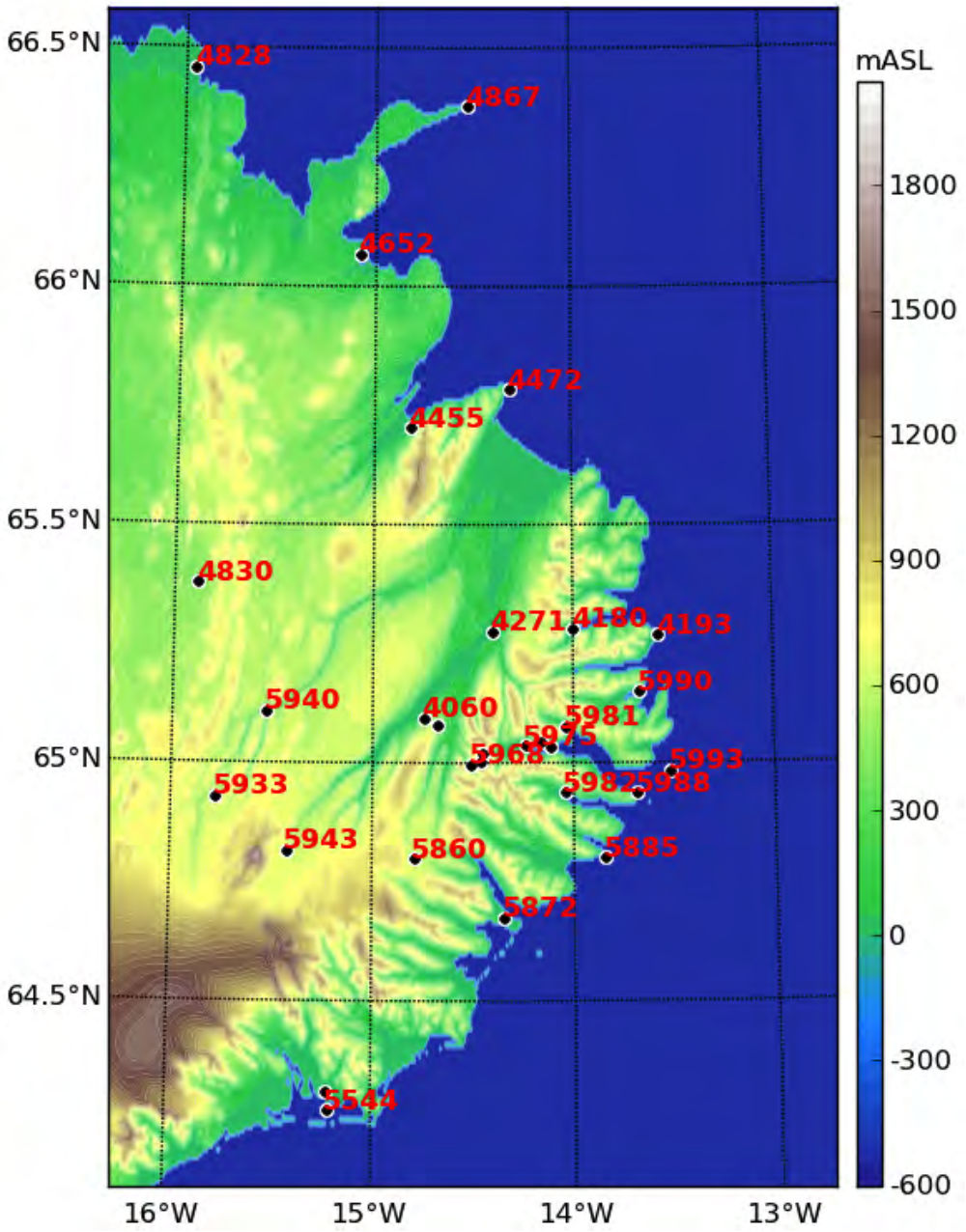


*Figure 5. Topography (based on the GLOBE digital terrain model) and locations of surface weather stations in eastern Iceland.*

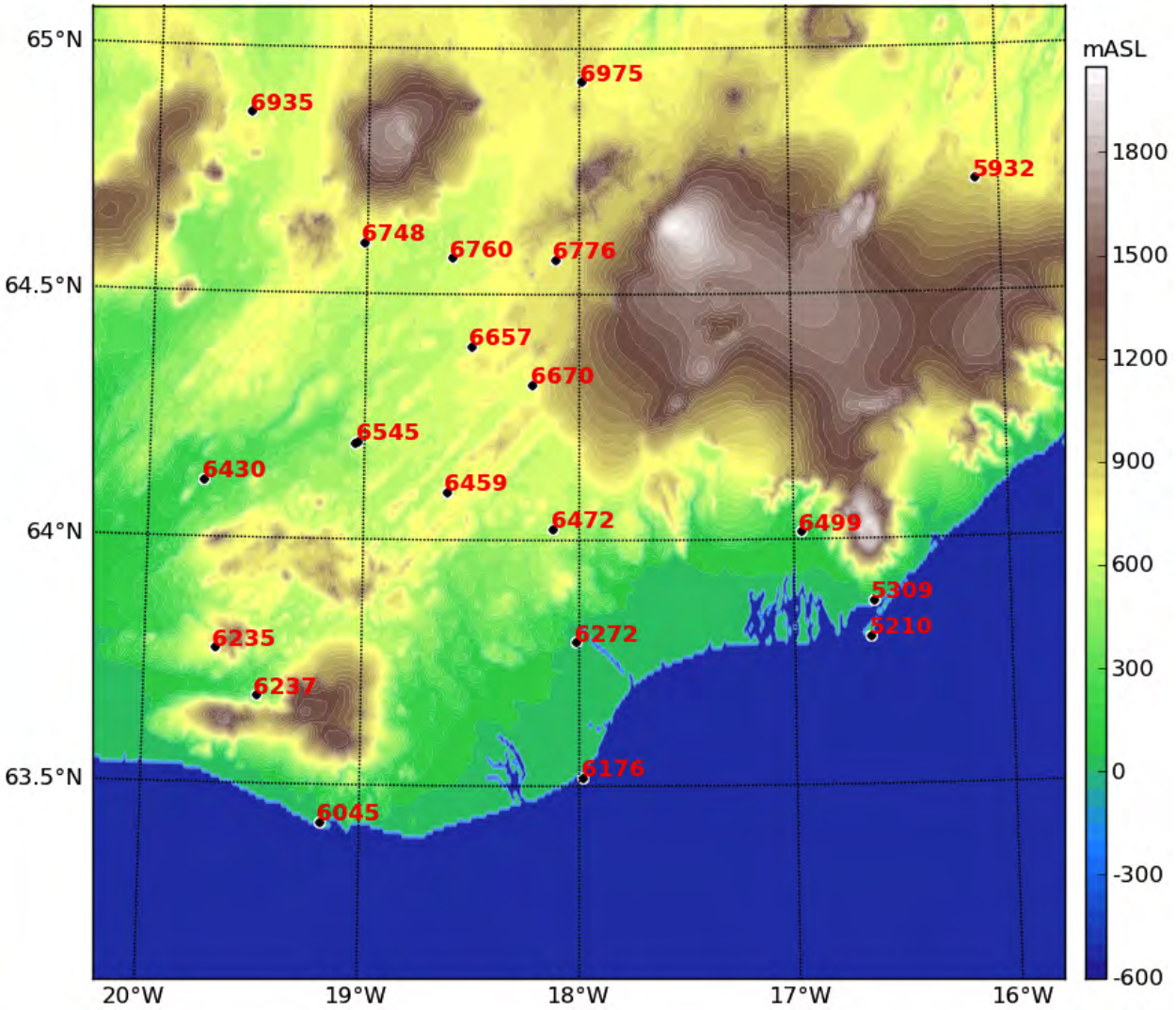


*Figure 6. Topography (based on the GLOBE digital terrain model) and locations of surface weather stations in southern Iceland.*

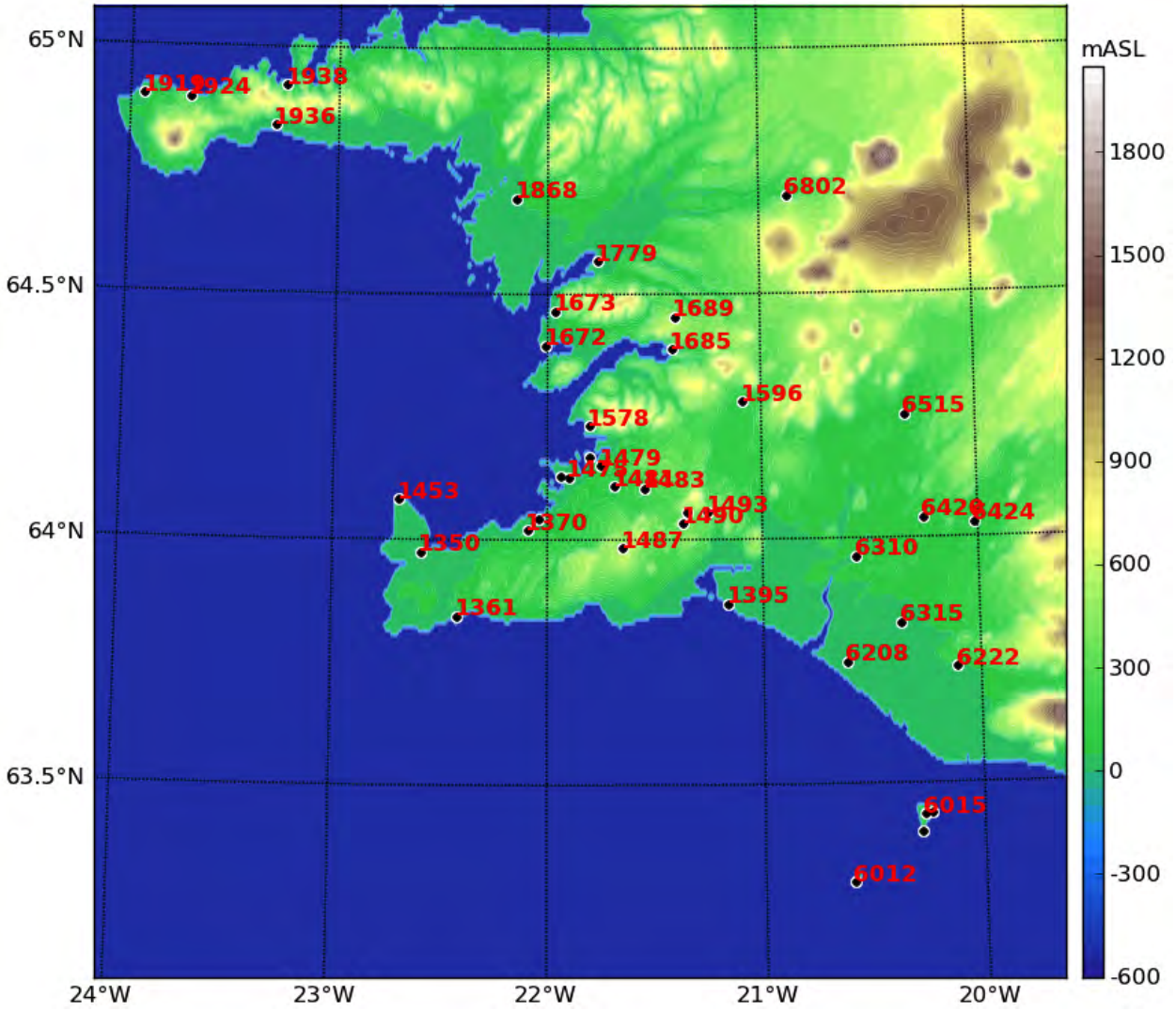


*Figure 7. Topography (based on the GLOBE digital terrain model) and locations of surface weather stations in southwest Iceland.*

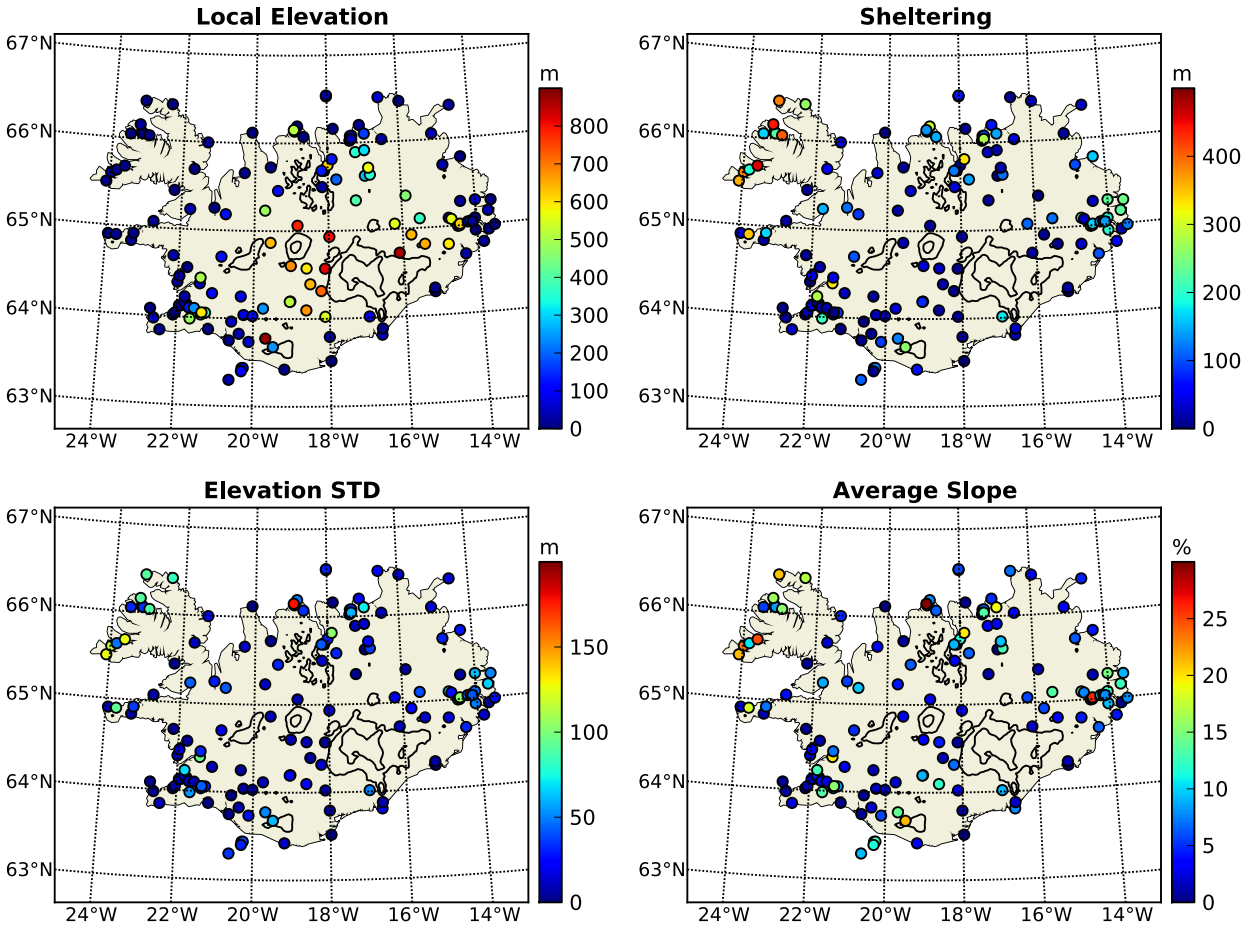


*Figure 8. Terrain statistics within 1 km around weather station locations derived from the Icelandic digital terrain model (see Section 3). Terrain elevation contour lines are drawn at 1000 and 1500 mASL.*

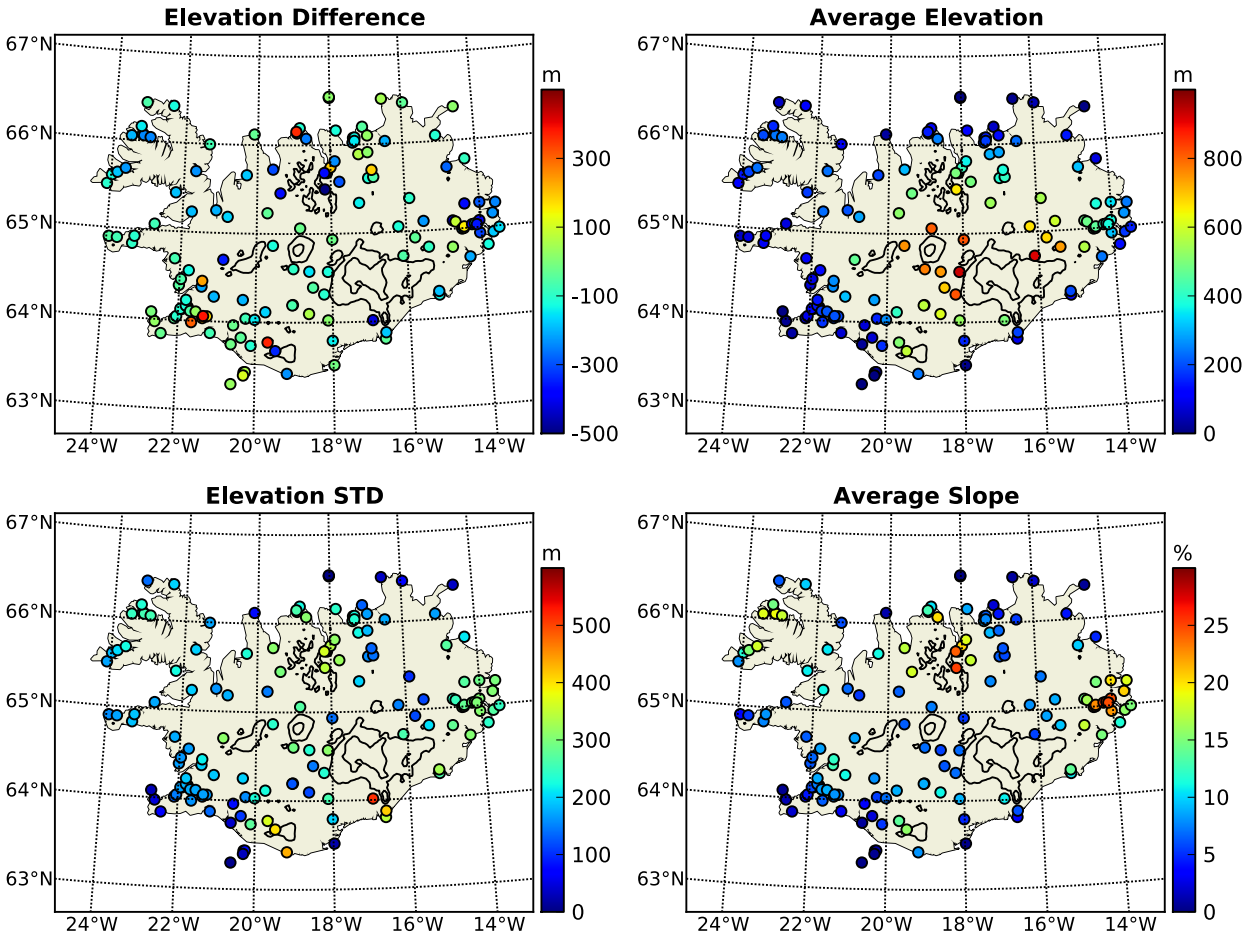


*Figure 9. Terrain statistics within 30 km around weather station locations derived from the Icelandic digital terrain model (see Section 3). Terrain elevation contour lines are drawn at 1000 and 1500 mASL.*

# 4 Methodology

This section describes different methods of deriving time-series at station locations from operational analysis fields, and the calculation of stereographic projections of horizontal wind vectors.

## 4.1 Selection of Local Values from Analysis Fields

For comparisons between operational analyses and surface station data, appropriate values, corresponding to individual station locations, need to be selected from the gridded fields. Generally, however, station locations do not coincide with any grid-point. For that reason, different selection methods are discussed in this section.

The representativeness of local values largely depends on the horizontal variability of meteorological fields, which varies greatly between different variables. For seasonally averaged fields of mean sea level air pressure (MSLP), shown in Figure 10, terrain effects are eliminated by the use of one reference level, resulting in fairly smooth wavelike spatial patterns. In winter, absolute pressure values are lower than in summer, with low pressure centres situated predominantly to the west-southwest of Iceland, and with the most intense pressure gradients over the western part of the island. In summer, the lowest pressure is found predominantly to the south-southwest of Iceland, with the strongest gradients along the northern coast. Correspondingly, geostrophic winds at mean sea level in winter are strongest in the west, with prevailing directions from the southeast. In summer, geostrophic winds weaken over the land, but intensify along the northern coast from east-northeasterly directions.

As shown in Figure 11, in contrast with MSLP, seasonally averaged analysis fields of surface wind speed have spatial patterns of well-defined maxima and minima over the land, which are inconsistent with those of the geostrophic wind at mean sea level, and must therefore be due to terrain effects as described in the ECMWF operational model. In fact, the highest wind speeds occur over the highest model terrain (see again Figure 2), whereas the the lowest wind speeds occur over the most rugged terrain of the island, as measured by regionally averaged terrain slope (see again Figure 9). Analysed surface wind speeds over the land are higher in winter than in summer. However, there is a proportionally greater wintertime increase in surface wind speed over the ocean. Consequently, especially in winter, there is a strong gradient between land and ocean grid-points. Due to the complex coastline of Iceland, several outlying land areas are not resolved by the ECMWF operational model. Most significantly, the western end of Snæfellsnes and the northern tip of the Westfjords are classified in analyses as ocean areas. Similarly, smaller islands off the southern and northern coast are not recognised by the operational model. In these places, the nearest land grid-point, for low- and high-resolution fields, is tens of kilometres away from station locations.

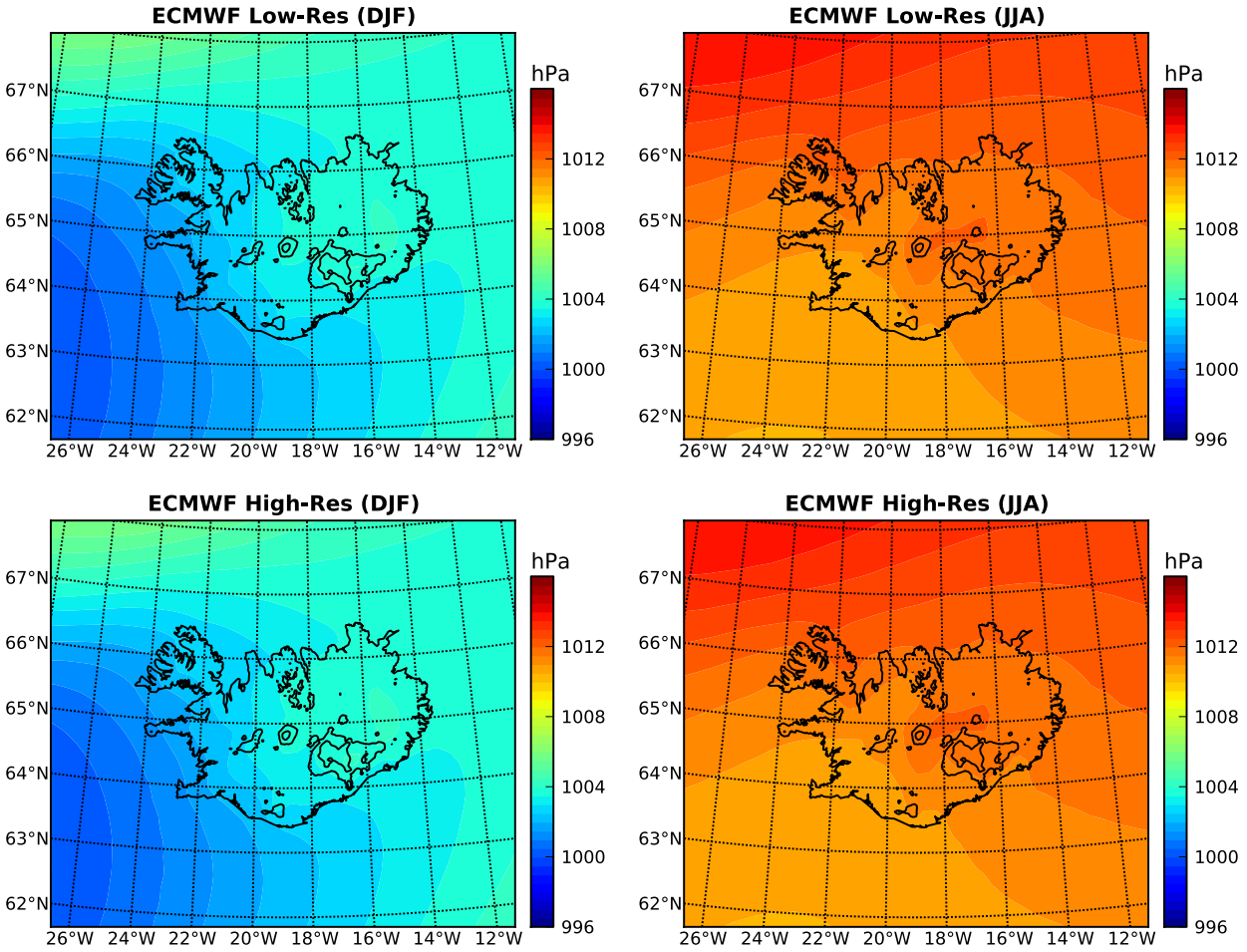


*Figure 10. Average mean sea level pressure in winter (DJF) and summer (JJA) based on low- and high-resolution operational analyses. Terrain elevation contour lines are drawn at 1000 and 1500 mASL.*

Surface air temperature, shown in Figure 12, also shows a clear dependence on model terrain elevation, with a strengthening of near-coastal gradients in winter.

The different selection methods for local values which were tested are:[2]
a) Linear interpolation from the four surrounding grid-points, taking into account only the relative distances from the weather station, regardless of land or ocean grid-points.
b) Choosing the value at the nearest land grid-point.
c) A mixed approach: If for a station location the surrounding four grid-points are either all over land or all over the ocean, according to the land–sea mask of the operational model, method a) is used; otherwise, method b).

A comparison between the results for annually averaged surface wind speed derived by the three different methods, using low-resolution analysis fields, is shown in Figure 13. There are no significant differences between linearly interpolated and nearest-neighbour values in the interior of

[2]Variations of method a) using different weights for land and ocean grid-points were tested and found to be of inconsistent value. Likewise, as a modification of method b), calculating the average between the nearest and the nearest land grid-point did not lead to general improvements.

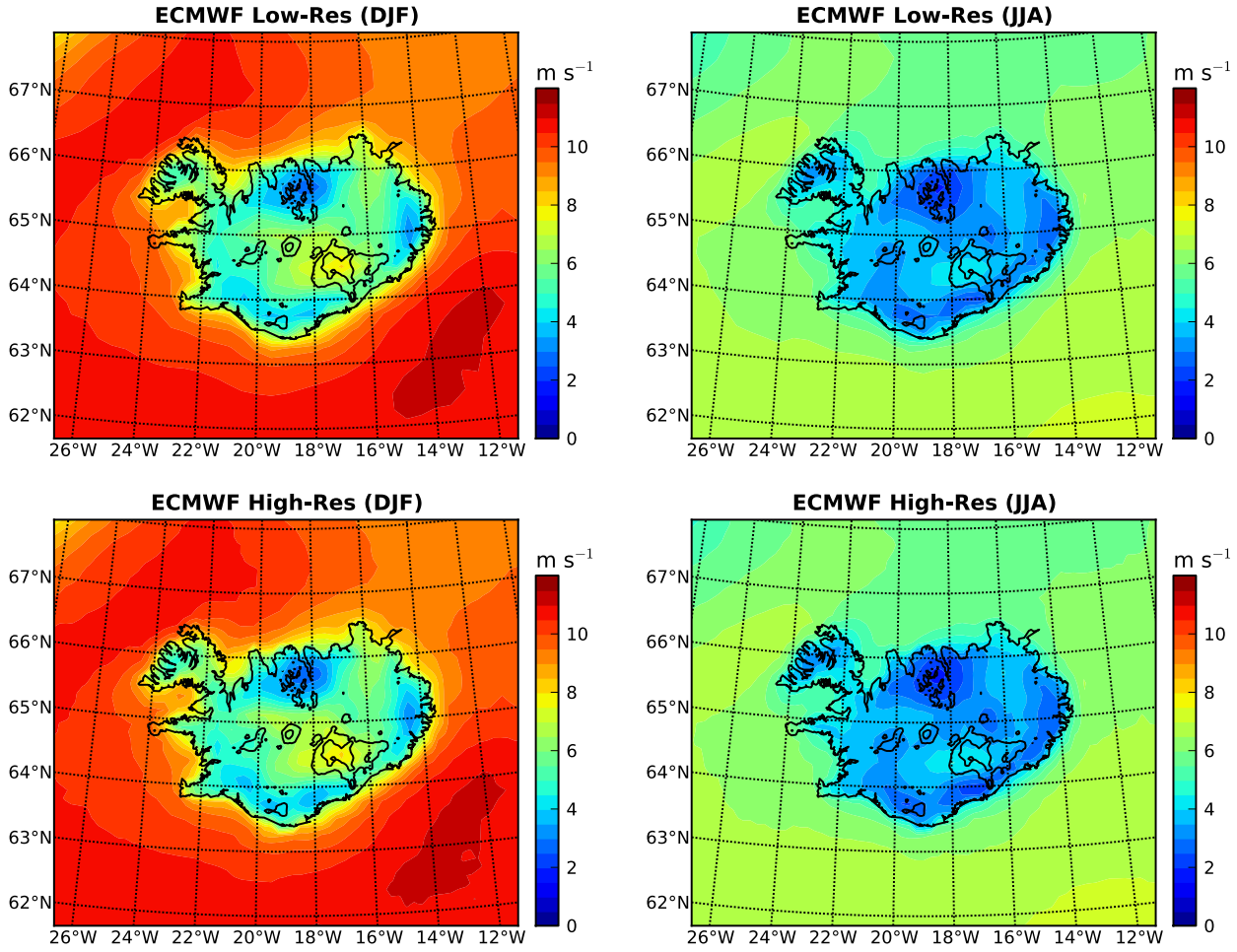


*Figure 11. Average surface wind speed in winter (DJF) and summer (JJA) based on low- and high-resolution operational analyses. Terrain elevation contour lines are drawn at 1000 and 1500 mASL.*

the island. As may be expected from Figure 11, on the western end of Snæfellsnes, and at the northern tip of the Westfjords, linearly interpolated values, using "off-shore" grid-points, are too large. Considering the other coastal locations, there is no bias towards either too high or too low values. By contrast, nearest-neighbour values along the coast are generally too low. The mixed method results in nearest-neighbour values north of Akureyri and east of Egilsstaðir, which are too low. However, too high linearly interpolated values on Snæfellsnes, at the northern tip of the Westfjords, and on Langanes in the northeast are maintained. For high-resolution analysis fields, there are only very few "coastal" locations with mixed land–ocean surrounding grid-points. The results then, at almost all station locations, are identical to linear interpolation. Overall, linear interpolation appears to provide the best results, and is employed throughout the rest of the analysis. Surface wind speed from operational analyses at station locations will always be referring to interpolated values from horizontal fields of wind speed, rather than the speed of interpolated wind vectors.

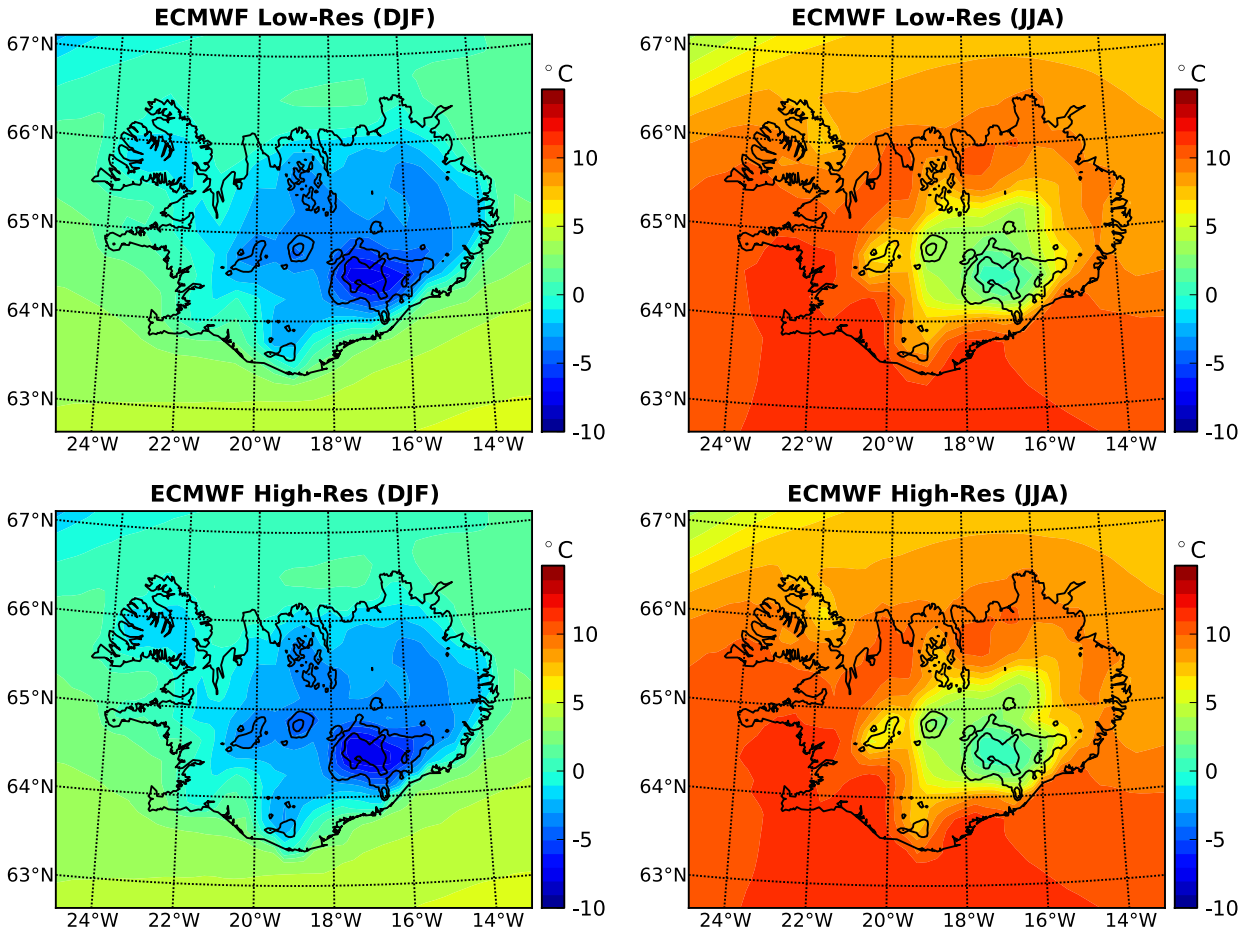


*Figure 12. Average surface air temperature in winter (DJF) and summer (JJA) based on low- and high-resolution operational analyses. Terrain elevation contour lines are drawn at 1000 and 1500 mASL.*

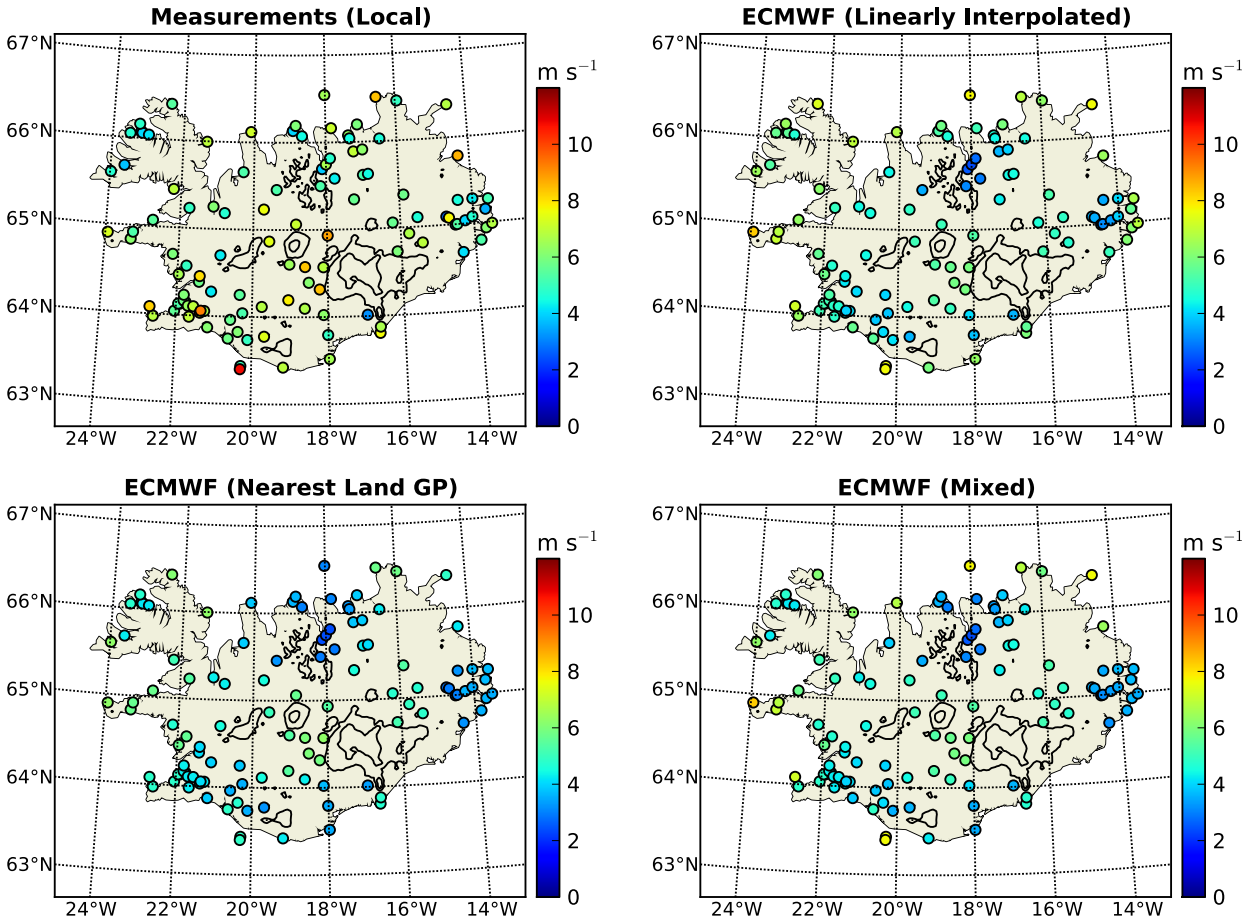


*Figure 13. Annually averaged surface wind speed at station locations for time-series of local measurements and low-resolution analysed values based on different interpolation methods (see Section 4.1).*

## 4.2 Stereographic Projection of Wind Vectors

For all maps presented here, a stereographic projection is used, requiring special consideration for the transformation of wind vectors.

On the curved surface of the Earth, the horizontal wind vector can be written as

$$\boldsymbol{v} = u\boldsymbol{i} + v\boldsymbol{j} \ , \tag{2}$$

with orthonormal unit vectors $(\boldsymbol{i}, \boldsymbol{j})$, oriented along the longitudinal and latitudinal coordinate axes, respectively, with corresponding velocity components $(u, v)$. Since stereographic projections are conformal, right angles between unit vectors are preserved. The projected wind vector on the flat figure plane can therefore still be written as

$$\boldsymbol{v}' = u'\boldsymbol{i}' + v'\boldsymbol{j}' \ , \tag{3}$$

where the new set of orthonormal unit vectors $(\boldsymbol{i}', \boldsymbol{j}')$ is derived by mapping stereographically the angular differentials $(d\lambda, d\phi)$, corresponding to $(\boldsymbol{i}, \boldsymbol{j})$, onto the vector differentials $(d\boldsymbol{x}', d\boldsymbol{y}')$ in the figure plane. The normalised unit vectors are then given by

$$\boldsymbol{i}' = \frac{d\boldsymbol{x}'}{|d\boldsymbol{x}'|} \tag{4}$$

$$\boldsymbol{j}' = \frac{d\boldsymbol{y}'}{|d\boldsymbol{y}'|} \ . \tag{5}$$

Additionally, the angles between the unit vectors $(\boldsymbol{i}, \boldsymbol{j})$ and $\boldsymbol{v}$ need to be preserved by the new unit vectors $(\boldsymbol{i}', \boldsymbol{j}')$ and $\boldsymbol{v}'$. This requires that

$$\frac{v'}{u'} = \frac{v}{u} \ . \tag{6}$$

Finally, it is required here that the projected wind vectors at different locations across the domain have the same relative lengths as in the original velocity field. This implies that

$$\sqrt{u'^2 + v'^2} = c\sqrt{u^2 + v^2} \ , \tag{7}$$

with an arbitrary positive scaling constant $c$. Together with (3) and (6), the projected wind vector is then given by

$$\boldsymbol{v}' = c\left(u\boldsymbol{i}' + v\boldsymbol{j}'\right) \ . \tag{8}$$

# 5 Seasonal Averages

For the purpose of comparison, in calculating local seasonal averages, for each missing value in surface station data, the corresponding value is removed from the time-series derived from operational analyses. No significant differences exist between seasonal averages based on either hourly or 6-hourly time-series (not shown).

## 5.1 Surface Wind

Local averages of hourly measured surface wind speeds in winter and summer are shown in Figure 14. Consistent with previous findings (Einarsson, 1984; Blöndal et al., 2011), winds are weaker in summer, due to weaker pressure gradients over the island (see again Figure 10). In winter and summer, generally the highest wind speeds are found over the interior highlands. In winter, intermediate and high measured wind speeds at low elevations also exist along the north and southwest coast. As pointed out by Einarsson (1984), by far the highest surface wind speeds are measured at the southernmost station on Vestmannaeyjar, due to its location on a low hill and near a cape on the mainland. Due to sheltering, the weakest measured winds in winter occur in the Westfjords and the eastern part of the island. In summer, the weakest winds are found in the Westfjords. Calculating averages for the cold season from September through April, and for the warm season from Mai through August, as well as projecting surface measurements to 90 mAGL using logarithmic vertical profiles, the same regional patterns of high and low wind speeds were found by Blöndal et al. (2011).

In winter, there are a few high-wind outliers compared with neighbouring stations, which can partly be explained by nearby terrain features. Station 1496 (Skarðsmýrarfjall) is located to the west of Station 1493 (Ölkelduháls), and somewhat higher up on Skarðsmýrarfjall (see Figures 7, 8, and 9). Station 6017 (Stórhöfði) is located to the south of Station 6015 (Vestmannaeyjabær), on a low hill at the southern tip of Heimaey, the main island of the Vestmannaeyjar archipelago (see Figure 7). It therefore has a greater exposure to strong off-shore winds. Station 5960 (Hallormsstaðaháls) is located on a ridge to the east-southeast of Station 4060 (Hallormsstaður) (see Figure 5).

In contrast, Station 6235 (Tindfjöll), located on the southwest slope of Tindfjöll (see Figure 6), experiences only a small increase in average wintertime wind speeds, despite the fact that it is situated about 700 m above the average regional elevation. Similarly, Station 3752 (Siglufjörður) is at a significantly higher local elevation than nearby Station 3754 (Siglunes) towards the northeast (see Figure 4). Nonetheless, it has a slightly weaker average wintertime surface wind speed due to its sheltered location at the head of Siglufjörður, compared with Station 3754, which is located at the open coast.

Figure 14 also shows the comparison between seasonal averages of measured surface wind speed and linearly interpolated values from low- and high-resolution operational analyses. Differences in seasonal averages between analysis fields with different resolutions are negligible. As for the annual averages discussed in Section 4.1, linearly interpolated analysed wind speeds, in winter and summer, on Snæfellsnes are too high, whereas in the interior, analysed speeds are almost exclusively too low, particularly in the Þórisvatn area west of Vatnajökull, as well as around Akureyri and east of Egilsstaðir.

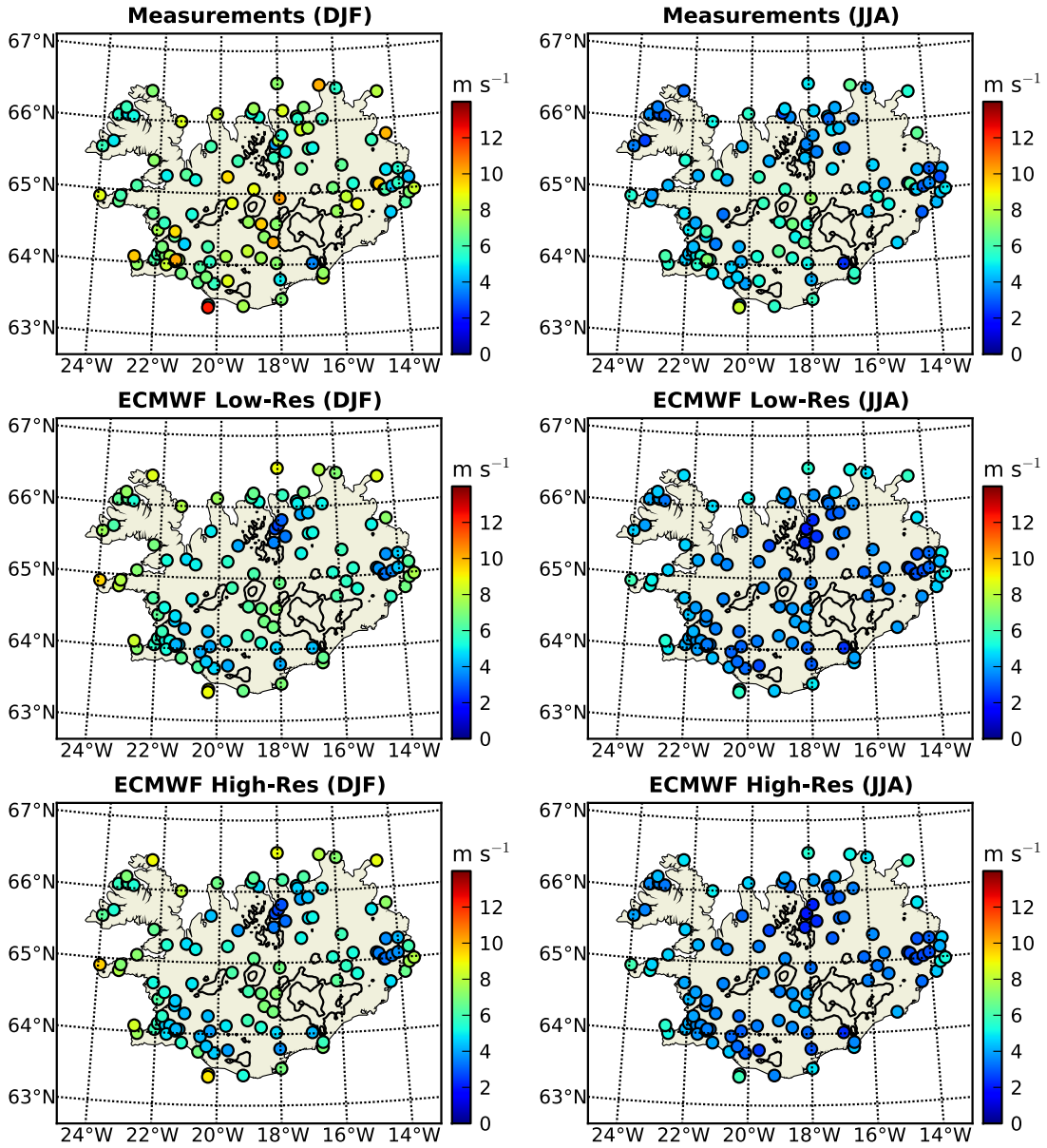


*Figure 14. Average surface wind speed in winter (DJF) and summer (JJA) based on local observational time-series and linearly interpolated operational analyses.*

Seasonally averaged measured surface wind vectors for low speeds ($2 \leq$ speed $< 5$ m s$^{-1}$) are shown in Figure 15. For weak winds, the influence of temperature gradients is clearly noticeable at nearly all locations (compare with Figure 12). Especially during winter, prevailing surface winds flow from low to high temperatures, downslope in the interior of the island, and off-shore along the coast. In summer, as seen in the following section, the surface air temperatures around Vatnajökull in the analyses are too low. Nonetheless, the reversal of land–sea temperature gradients compared with winter along the coast is well represented, and results in prevailing on-shore winds in most places. This has previously been discussed by Einarsson (1984). Exceptions are found at outlying locations in the north, where east-northeasterly surface winds are affected by large-scale pressure gradients (shown in Figure 10), as well as in the southwest region, where summertime temperature gradients are weak.

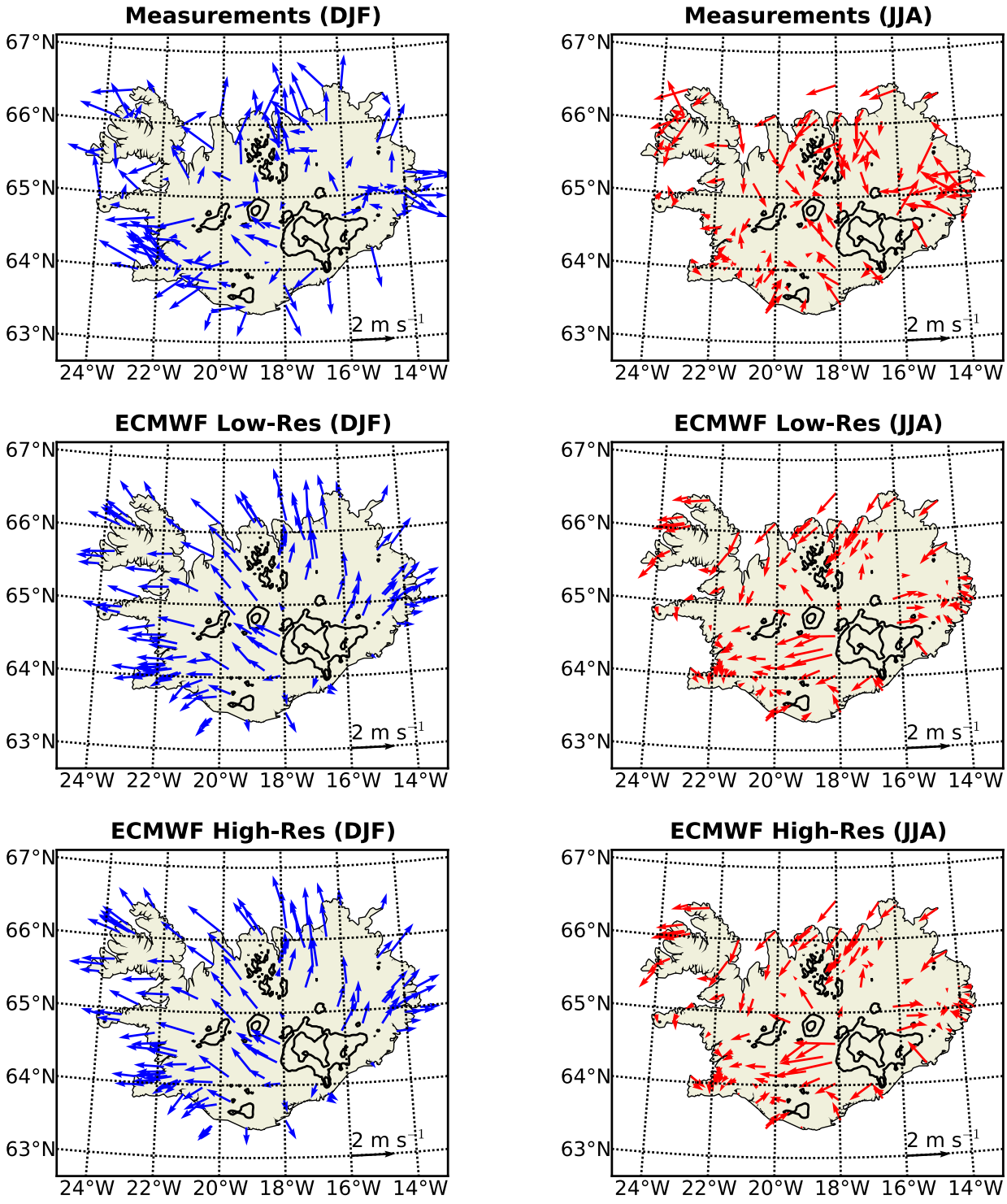


*Figure 15. Average surface wind vectors in winter (DJF) and summer (JJA) based on local observational time-series and linearly interpolated operational analyses, taking into account low surface wind speeds ($2 \leq$ speed $< 5$ m s$^{-1}$).*

For intermediate and high measured surface wind speeds (speed $\geq 5$ m s$^{-1}$), in both seasons, strong easterly and southeasterly winds dominate near the coast in the western part of the island (see Figure 16), where large scale geostrophic winds combine with local temperature gradients (refer again to Figures 10 and 12). Inconsistency between large-scale and local forcing in the east results in weaker average wind vectors. The largest seasonal difference in intermediate to strong surface winds is found in the region south of Húnaflói (east of the Westfjords), where wind direction variability in summer is reduced in favour of a higher occurrence of on-shore northerly winds. In the Mývatn area in the northeast, a change occurs from southerly off-shore winds in winter, to northerly on-shore winds in summer.

As for wind speed, differences in seasonally averaged wind vectors derived from operational analysis fields with different resolutions are negligible. In winter, the prevailing weak to strong off-shore flow is well represented in the analyses. In summer, weak to strong winds along the northern coast have a too large northerly component, while there are too strong easterly average winds in the Þórisvatn area.

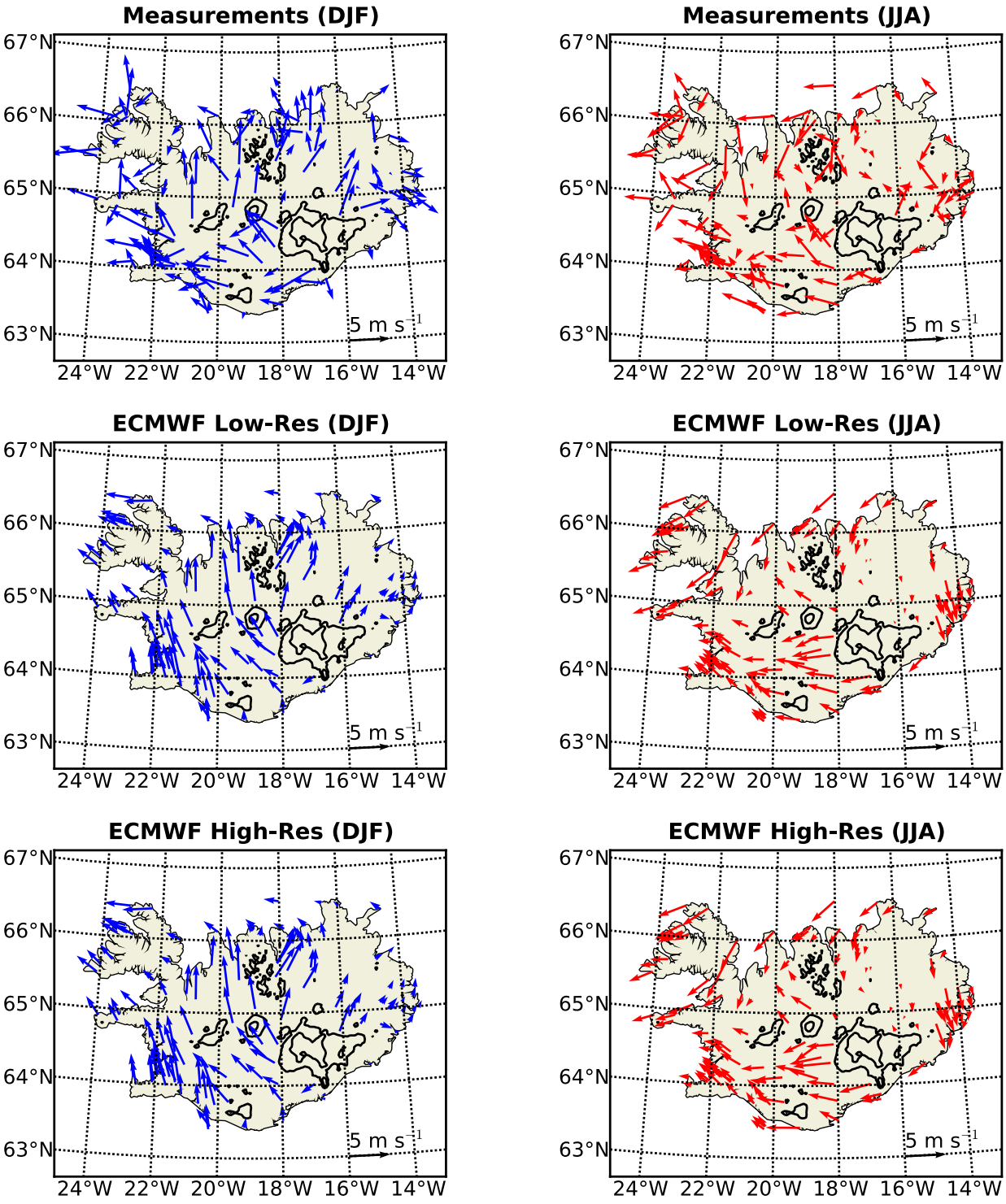


*Figure 16. Average surface wind vectors in winter (DJF) and summer (JJA) based on local observational time-series and linearly interpolated operational analyses, taking into account intermediate to high surface wind speeds (*speed $\geq 5$ m s$^{-1}$*).*

## 5.2 Surface Air Temperature

Local and regional averages of surface air temperature in winter and summer are shown in Figure 17. These results are qualitatively consistent with those obtained by Björnsson et al. (2007) and Crochet and Jóhannesson (2011), although different periods were analysed in those studies. Contrary to surface wind speed, there are no significant outliers. In winter and summer, the lowest measured temperatures exist in the interior of the island. In winter, temperatures along the coast vary little, with only slightly higher values in the south. In summer, the highest temperatures at low elevations are found in the southwest. As for surface wind, there are no significant differences between seasonal averages derived from operational analysis fields with different spatial resolutions. In the interior, the seasonal cycle is too weak compared with measurements, primarily due to too high wintertime temperatures.

In the previous subsection, the connection between surface air temperature gradients and surface winds was discussed in relation to the seasonal reversal of near coastal wind directions. Complementary to this, differences in surface air temperature during either on- or off-shore wind conditions will be discussed here. For this, that component of the local wind vector is calculated, that points into the direction from the station location to 18.35°W and 64.77°N, located halfway between Hofsjökull and Vatnajökull, approximately in the centre of the island. Wind conditions at each individual location are then separated into cases in which the inland component of the local wind vector is either positive or negative. Additionally, for comparison with surrounding surface air temperatures and sea surface temperatures, operational analysis fields are separated into cases during which the average of the inland component of the wind vector at all locations below 100 mASL is either positive or negative. For each class of wind conditions, the average surface air temperature at each station location for winter and summer is then calculated.

The results for averages based on station data are shown in Figure 18, whereas Figure 19 shows the results for station averages based on low-resolution operational analyses. As Einarsson (1984) pointed out, surface air temperatures over Iceland are strongly influenced by large temperature differences between the surrounding ocean currents. The Irminger Current, a branch of the warm North Atlantic Drift, encircles the western half of the island, while the East Icelandic Current, a branch of the cold East Greenland Current, passes southward along the east coast. It is found here that, in winter, the coldest temperatures over land are situated further northeast with on-shore than with off-shore winds. Also, the temperatures in the southwest are significantly warmer with on-shore winds. These changes are well represented in the operational analyses.

This increase in the northeast to southwest temperature gradient across the island with on-shore winds is consistent with differential temperature advection associated with the north to south gradient in air and sea surface temperatures. Northerly onshore winds lower surface air temperatures over the northern half of the island, whereas southerly onshore winds increase temperatures over the southern half of the island. With offshore winds from the elevated interior of the island, temperatures along the coast are more homogeneous. Based on the operational analyses, relatively cold off-shore flow is seen to extend several kilometres over the ocean. In summer, low-elevation measured and analysed surface air temperatures near the coast are very similar to the surrounding sea surface temperatures. Consequently, there is no significant impact on average land-based temperatures from winds with either on- or off-shore directions.

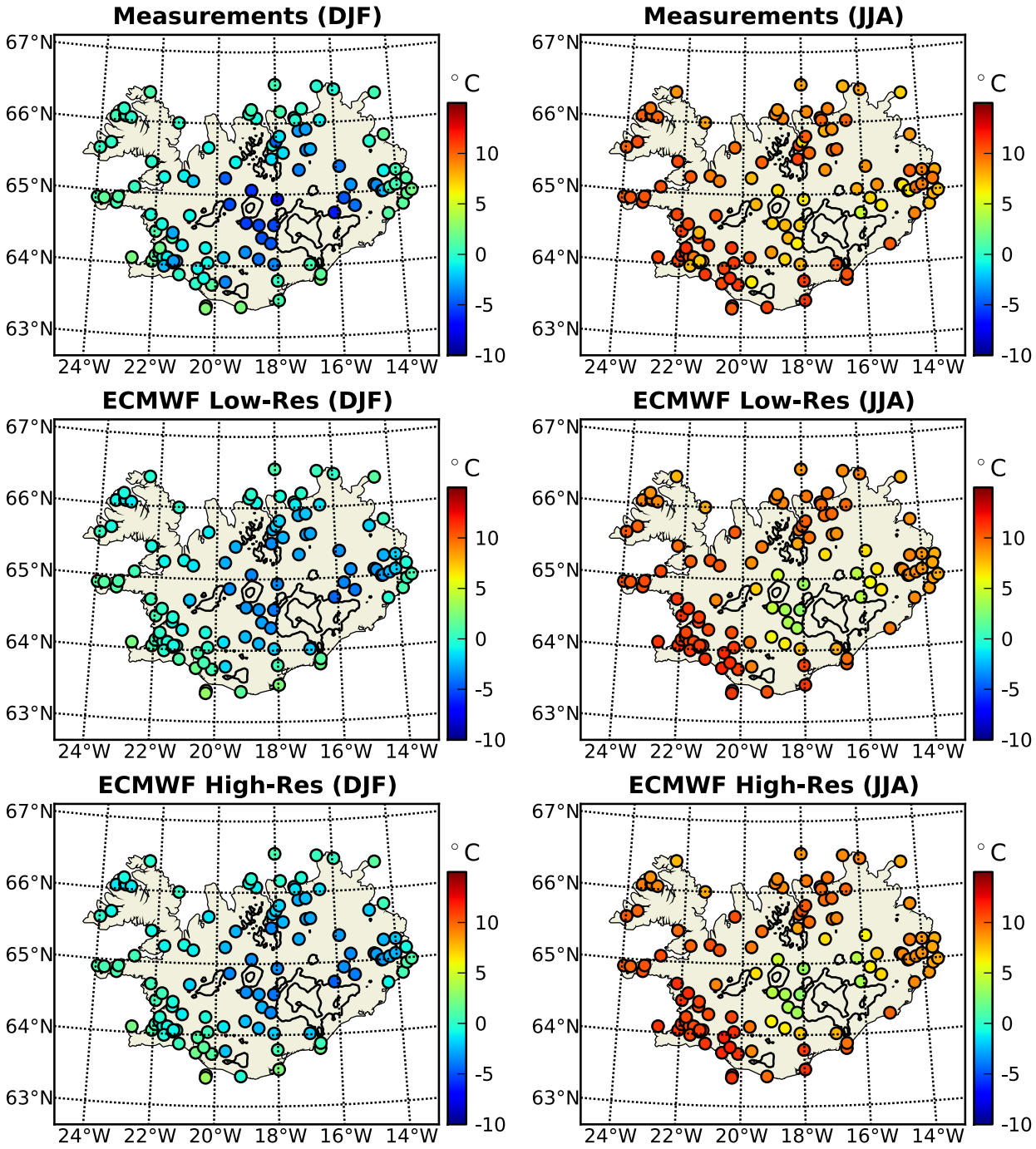


*Figure 17. Average surface air temperature in winter (DJF) and summer (JJA) based on local observational time-series and linearly interpolated operational analyses.*

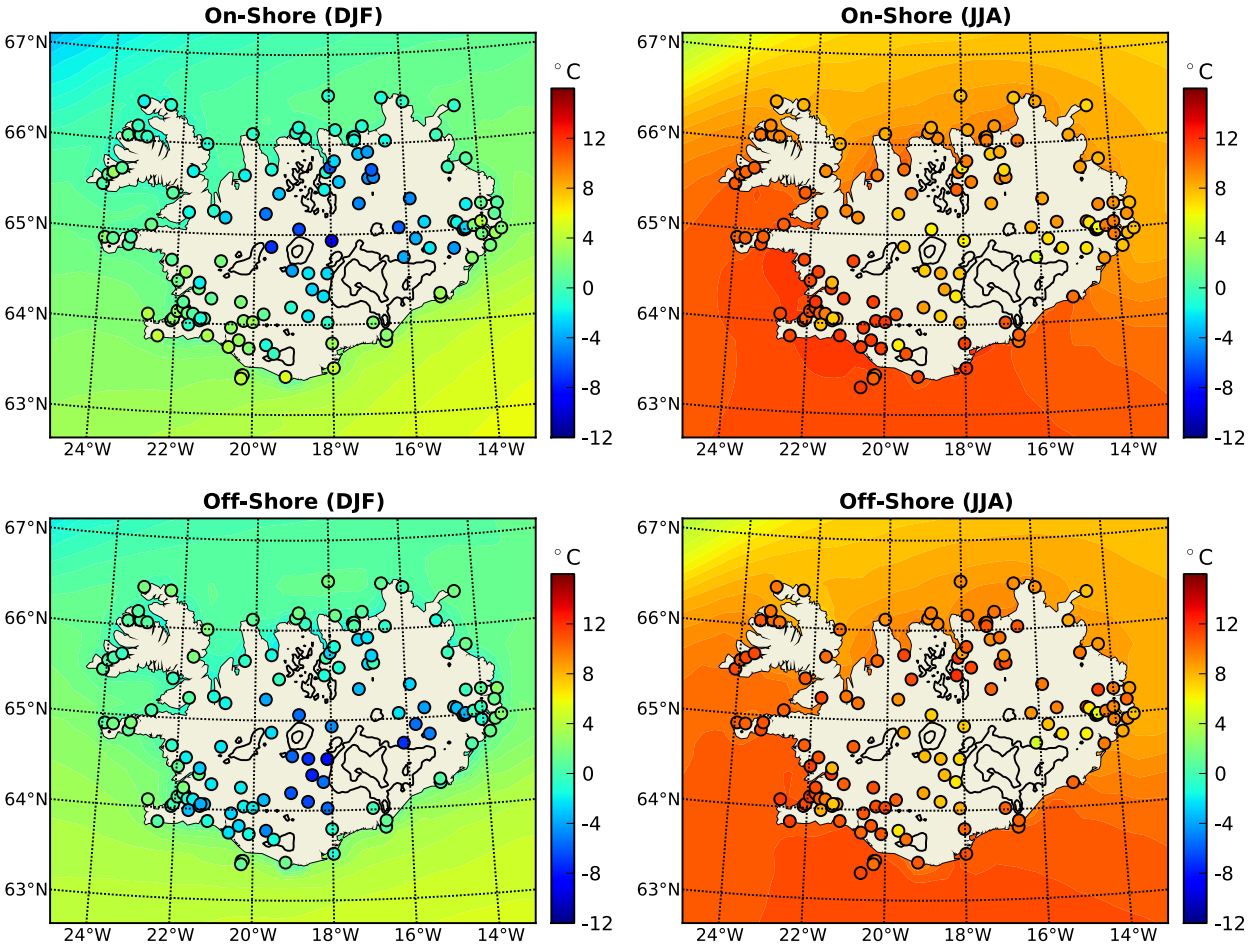


*Figure 18. Average land surface air temperature (coloured dots) in winter (DJF) and summer (JJA) at station locations for local observational time-series, and average surface air temperature over the ocean from high-resolution operational analyses, separated into cases with on-shore or off-shore surface winds (see Section 5.2).*

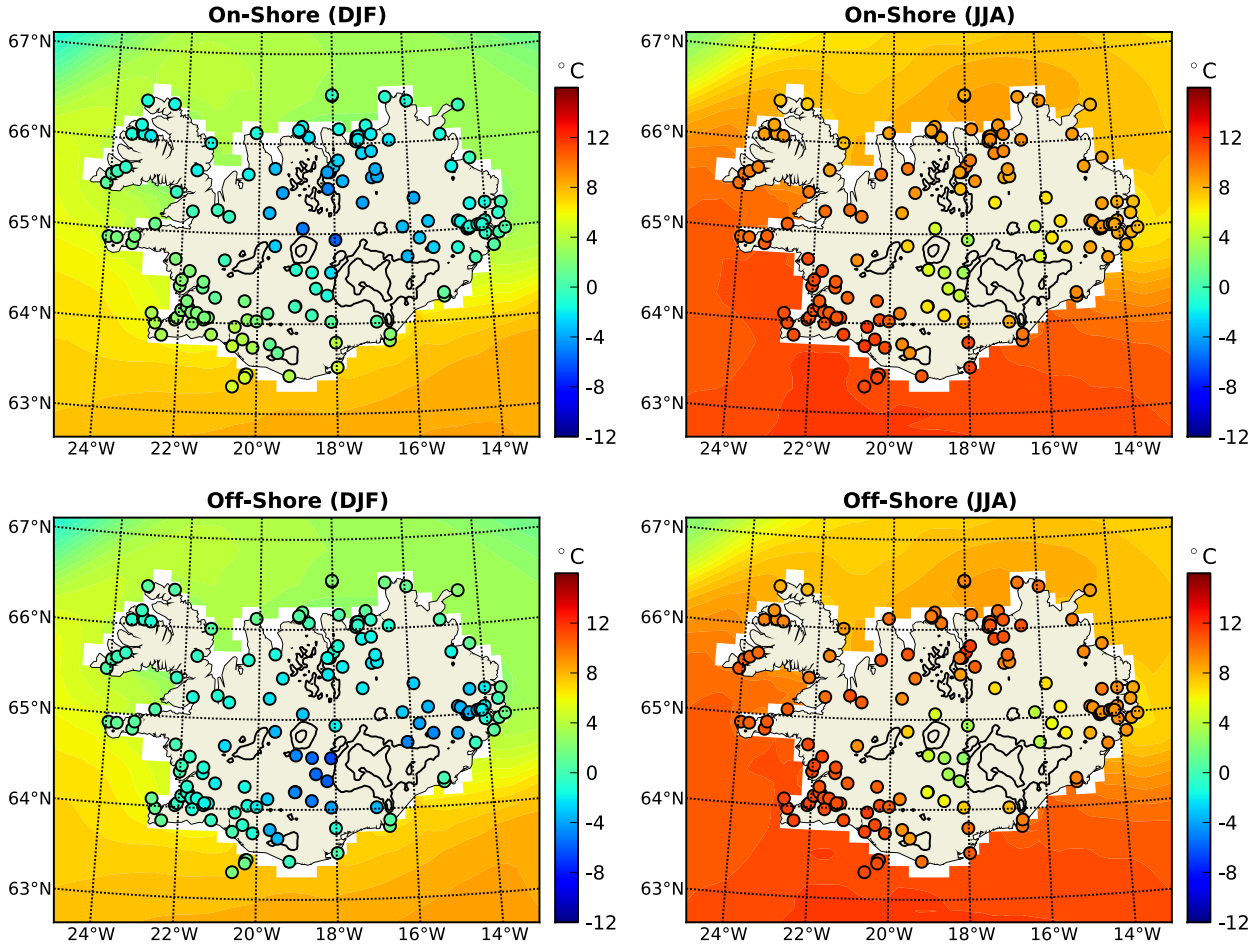


*Figure 19. Average land surface air temperature (coloured dots) in winter (DJF) and summer (JJA) at station locations for linearly interpolated low-resolution operational analyses, and average sea surface temperature from high-resolution operational analyses, separated into cases with on-shore or off-shore surface winds (see Section 5.2).*

# 6 Temporal Variability

A meaningful characterisation of inter-annual variability requires longer time-series than those used in this study. Therefore, the seasonal cycle is the longest dominant mode of variability resolved in the data record.

For surface air temperature, the magnitude of the seasonal cycle can easily be quantified by taking the difference between summer and winter averages. In contrast, as seen below, for surface wind speed, generally two maxima of monthly mean values occur in spring and autumn. However, this is not consistently the case throughout the island. Therefore, as a generally applicable measure of the magnitude of the seasonal cycle of any variable, the standard deviation of monthly averages throughout the year will be used. Complementary, the measure of variability on sub-monthly time-scales, or time-scales of transient weather systems, is defined as the average of standard deviations for each individual month. With the average and standard deviation over any sequence of numbers denoted by $E[\ ]$ and $D[\ ]$, respectively, and with monthly averages and standard deviations over a given time-series $S_i$, at the $i$-th location, denoted by $E_m[S_i]$ and $D_m[S_i]$, these two measures of variability are formally defined as

$$A[S_i] = D[E_m[S_i]] \tag{9}$$

for seasonal variability, and

$$M[S_i] = E[D_m[S_i]] \tag{10}$$

for sub-monthly variability. No significant differences exist for these two measures of variability between either hourly or 6-hourly time-series.

Finally, on the shortest resolved time-scale, that of the sampling rate, temporal variability is defined as root mean square tendencies,

$$R[S_i] = \Delta^{-1}\sqrt{E\left[\left(S_i(t+\Delta) - S_i(t)\right)^2\right]}\ , \tag{11}$$

where $\Delta$ is the time interval between subsequent data points (6 hours in this study). For time-series of wind direction, which have discontinuities around north, the differences $(S_i(t+\Delta) - S_i(t))$ in degrees are reduced to the half-open interval $(-180, 180]$.

## 6.1 The Seasonal Cycle

For the calculation of seasonal cycles of surface air temperature and surface wind speed, stations are separated either by local terrain elevation, or by geographical region.

According to terrain elevation, $z_s$, stations are classified as

- low coastal for $0 \leq z_s < 15$ m,
- high coastal for $15 \leq z_s < 50$ m,
- intermediate for $50 \leq z_s < 400$ m,
- high for $z_s \geq 400$ m.

According to longitude, $\lambda_s$, and latitude, $\phi_s$, stations are classified as belonging to

- the northwest region for $\lambda_s < -18°$E and $\phi_s \geq 65°$N,
- the northeast region for $\lambda_s \geq -18°$E and $\phi_s \geq 65°$N,
- the southwest region for $\lambda_s < -18°$E and $\phi_s < 65°$N,
- the southeast region for $\lambda_s \geq -18°$E and $\phi_s < 65°$N.

Thereby, to avoid biases due to different numbers of inland and coastal stations within different regions, as well as different numbers of low- and high-elevation stations, for the regional classification only stations with local elevations below 50 mASL are used. These stations invariably are near the coast.

Ensemble averaged seasonal cycles of surface air temperature for stations separated according to local terrain elevation, based on measurements and operational analyses, are shown in Figure 20. At all elevations, the lowest monthly temperatures occur in February, and the highest in July, although near the coast, August remains almost as warm. As for seasonal averages, differences between monthly ensemble averages derived from analyses with different spatial resolutions are negligible. At low elevations up to 50 mASL, on average, analysed winter temperatures are slightly too low. At intermediate elevations, where measured winter temperatures are about 1 K lower than at low elevations, there is a close match between observations and analyses. At elevations above 400 mASL, overall and especially wintertime measured temperatures are several degrees lower than at the coast. As seen before, based on operational analyses, the magnitude of the seasonal cycle is too small, with slightly too cold summer temperatures, and too warm winter temperatures.

Ensemble averaged seasonal cycles of surface air temperature for stations separated according to region are shown in Figure 21. As can be seen from this regional comparison, the too low wintertime temperatures in the analyses for low-lying stations (as seen in the previous figure), are mostly due to locations in the north. Low-elevation summer temperatures are around 10°C in July and August, with the exception of the southwest region, where monthly temperatures in July peak at about 12°C. The lowest winter temperatures in February are about 1–2 degrees lower in the northern part of the island, compared with the south.

Ensemble averaged seasonal cycles of surface wind speed for stations separated according to local terrain elevation are shown in Figure 22. At low elevations near the coast, there are only small differences between ensemble averages of observations and operational analyses. On average, below 400 mASL, surface wind speeds are 4 m $s^{-1}$ in summer, and around 6 m $s^{-1}$ in autumn and winter. Above 400 mASL, there is a noticeable increase in ensemble averaged measured wind speed. At those higher elevations, consistent with the results discussed in the previous section, analysed wind speeds are consistently too low. The timing of the lowest and highest wind speeds, on average, is the same at all elevations, and well represented by the analyses.

As seen in Figure 23, at low elevations, there are no significant differences in ensemble averaged surface wind speeds between different regions.

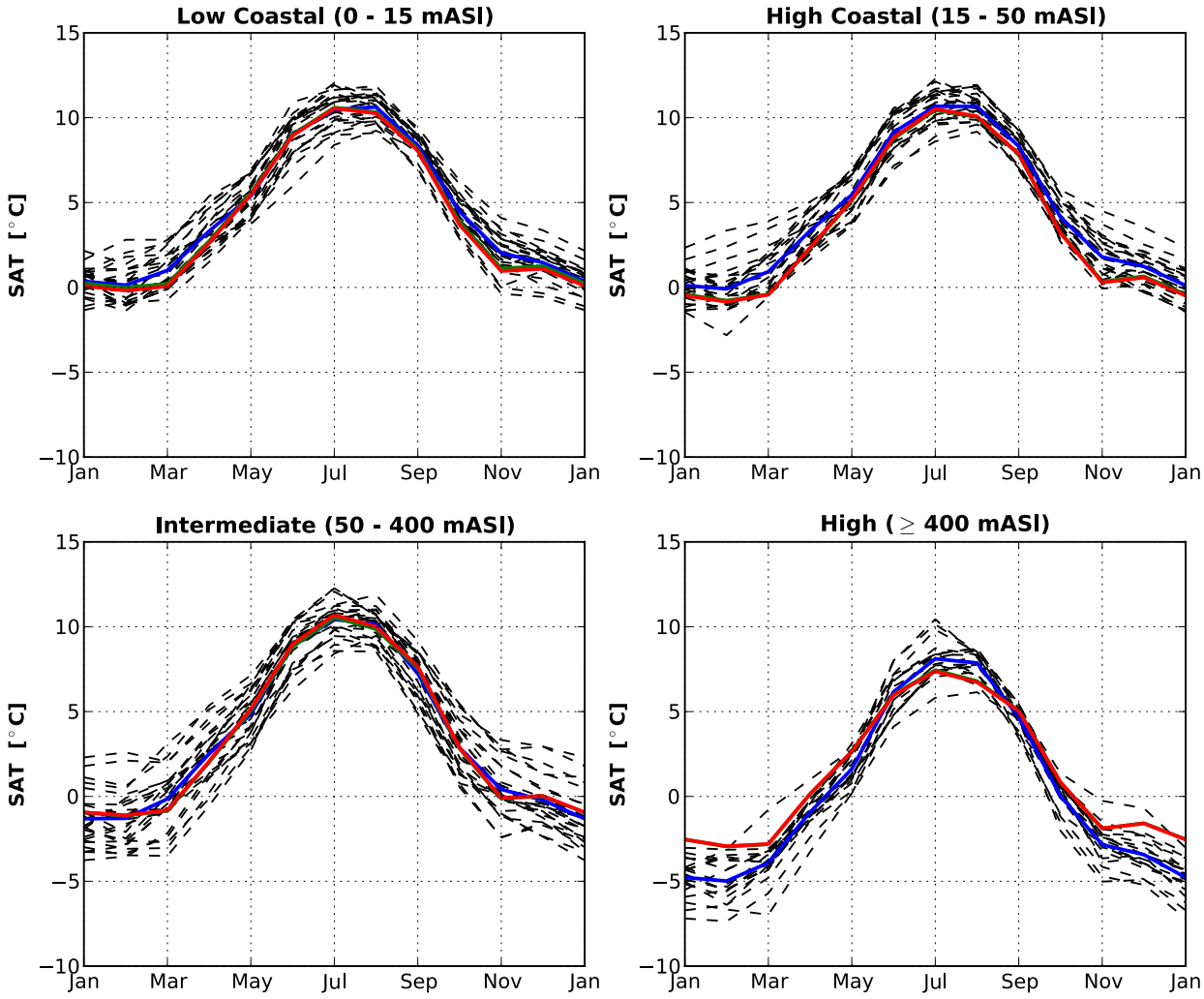


*Figure 20. Seasonal cycle of surface air temperature at different locations (dashed black lines), classified according to station elevation. Also shown are ensemble averages within each group for observations (blue lines), and high-resolution analyses (red lines). Results for low-resolution analyses (green lines) are mostly hidden by those for high-resolution analyses.*

## 6.2 Surface Wind

Temporal variability on seasonal and sub-monthly time-scales of surface wind speed based on station data and operational analyses, is shown in Figure 24. On a seasonal time-scale, there is no consistent spatial pattern in temporal variability, although the highest values are found at the coast. On shorter time-scales up to one month, with the exception of a few high-variability outliers at the coast, variability generally decreases from the centre of the island outwards. The main high-variability outlier on a sub-monthly time-scale is Station 6017 (Stórhöfði), situated (as mentioned in Section 5.1) on a low hill on the southern tip of Heimaey. This station not only has the highest average surface wind speeds, but is also in the region with typically the lowest mean sea level pressure throughout the year (refer again to Figure 10). The high temporal variability of surface wind speed on short time-scales is therefore most likely related to cyclone activity. Differences

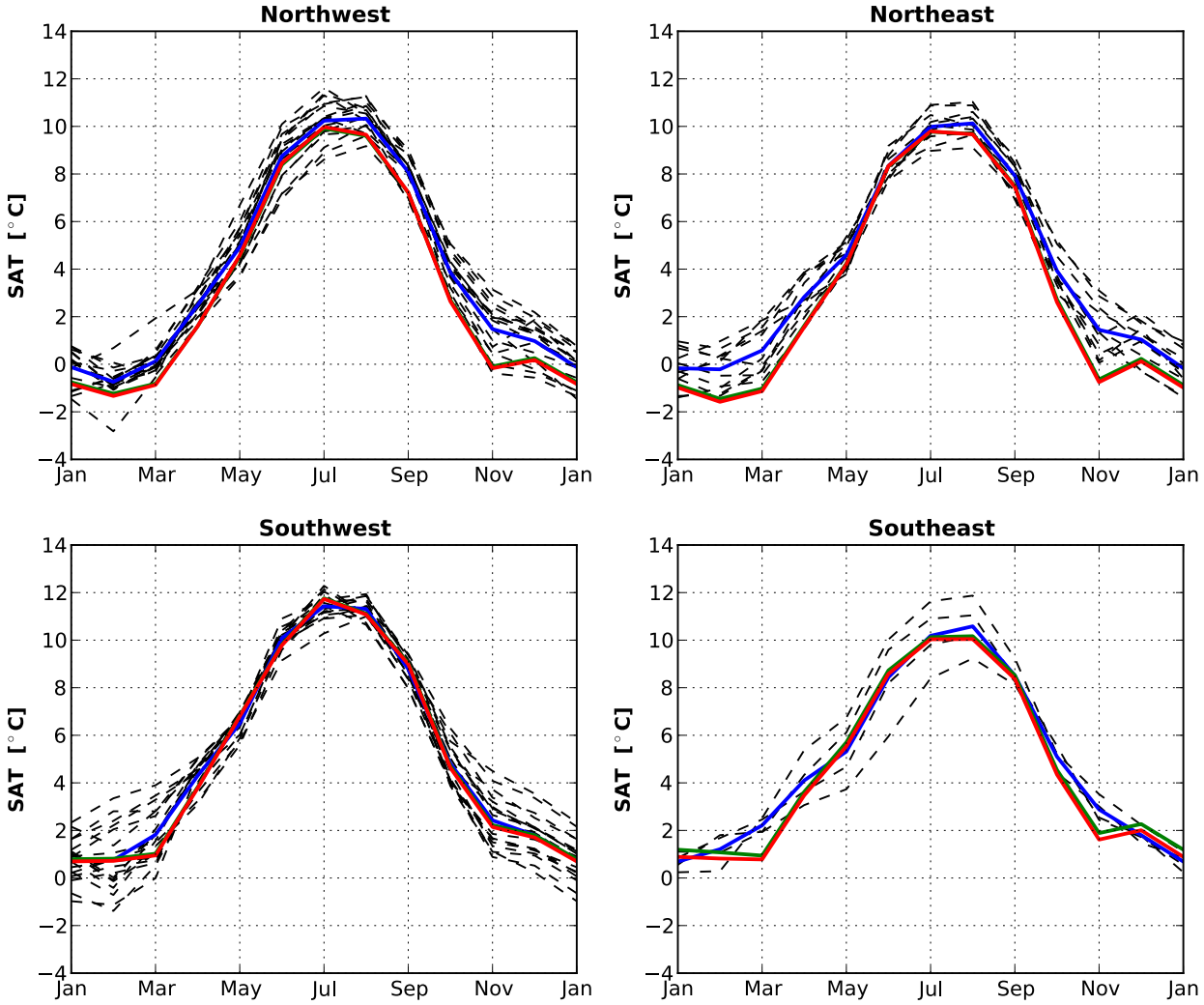


*Figure 21. Seasonal cycle of surface air temperature at different locations (dashed black lines), classified according to region. Also shown are ensemble averages within each group for observations (blue lines), and high-resolution analyses (red lines). Results for low-resolution analyses (green lines) are mostly hidden by those for high-resolution analyses.*

between variability derived from analysis fields with different spatial resolution, on both time-scales, are negligible. On a seasonal time-scale, variability is well-represented in analyses, as far as spatial patterns are concerned, although the seasonal cycle is underestimated in the southwest and the Mývatn area. One high-variability outlier is Station 2862 (Hornbjargsviti), located at the northern tip of the Westfjords. The large annual cycle there is overestimated in analyses, and largely driven by oscillations in the intensity of off-shore winds to the northwest of Iceland (see Figure 11). On sub-monthly time-scales, analysed temporal variability is generally too low, especially in the interior where, as discussed in Section 5.1, also seasonally averaged surface wind speeds are underestimated.

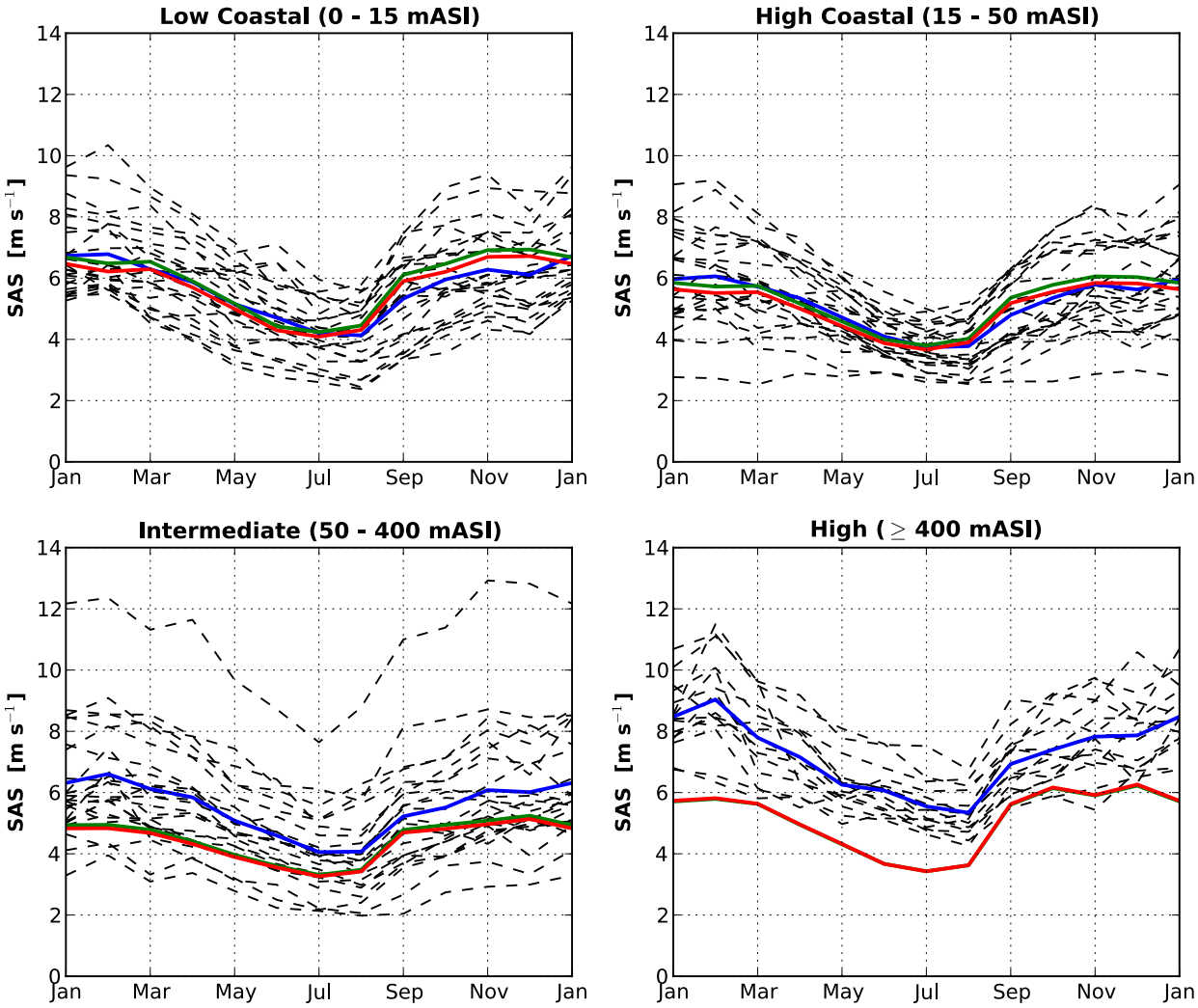


*Figure 22. Seasonal cycle of surface wind speed at different locations (dashed black lines), classified according to station elevation. Also shown are ensemble averages within each group for observations (blue lines), low-resolution analyses (green lines), and high-resolution analyses (red lines).*

As shown in Figure 25, root mean square tendency (RMST) of measured surface wind direction generally decreases with wind speed, although at some locations, wind direction variability increases again at high speeds. This increase is also seen at many coastal locations in the operational analyses, especially in winter.

Some consistent regional differences exist for wind direction variability. For low surface wind speeds ($2 \leq$ speed $< 5$ m s$^{-1}$), this is shown in Figure 26. In winter, the wind direction variability is lowest on Reykjanes and to the southeast of the peninsula, whereas the highest values are found around Egilsstaðir, Akureyri, and in the Westfjords. In summer, wind direction variability generally increases throughout the island, as diurnally oscillating thermal wind systems become more important.

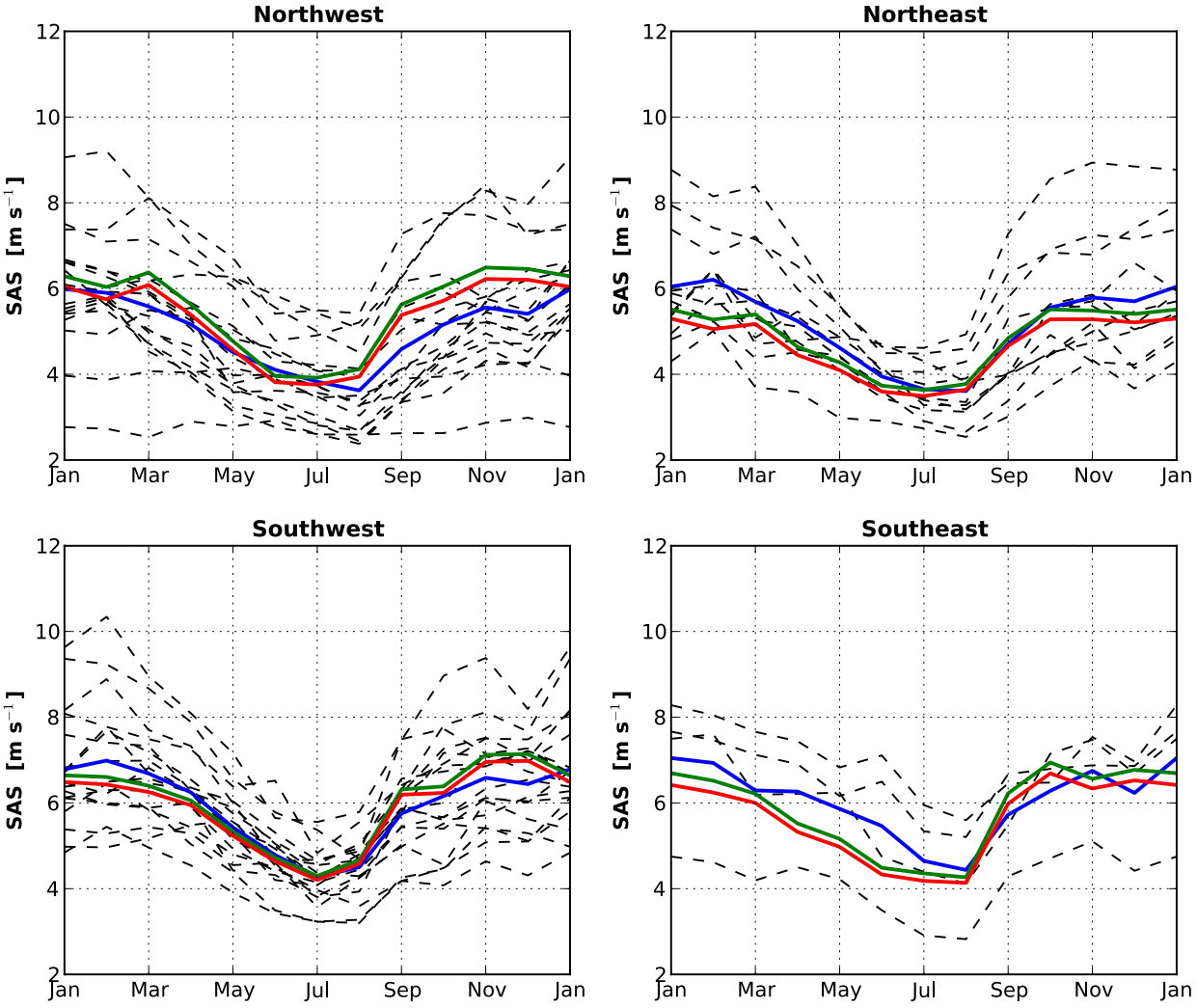


*Figure 23. Seasonal cycle of surface wind speed at different locations (dashed black lines), classified according to region. Also shown are ensemble averages within each group for observations (blue lines), low-resolution analyses (green lines), and high-resolution analyses (red lines).*

As shown in Figure 27, for intermediate and high surface wind speeds (speed $\geq 5$ m s$^{-1}$), wind direction is generally more steady than for weak winds. In winter, there are no significant regional patterns. In summer, locations with high wind direction variability are primarily within 30 km of the coast. One high-variability outlier in summer is Station 6499 (Skaftafell), situated in a sheltered location at the southern edge of Vatnajökull, with low seasonally averaged wind speeds. The neighbouring station to the southeast is Station 5309 (Fagurhólsmýri), where summertime wind speeds are greater by a factor of 6. Intermediate winds at Station 6499 generally coincide with strong winds at the nearest station. Therefore, shear induced turbulence, related to the elevated terrain, is likely to be the cause for the high wind direction variability.

## 6.3 Surface Air Temperature

Temporal variability on seasonal and sub-monthly time-scales of surface air temperature based on station data and operational analyses, is shown in Figure 28. As is expected, measurements show that the seasonal cycle is largest in the centre of the island, and decreases towards the coast. Variability on shorter time-scales of up to one month is highest in the region of relatively flat terrain between Mývatn and the northern slopes of Vatnajökull. Qualitatively, these results are consistent with those found by Gylfadóttir (2003) and Björnsson et al. (2007), although in these studies different measures of temporal variability within a different time period were used. As seen in Sections 5.2 and 6.1, operational analyses greatly underestimate the seasonal cycle in surface air temperature in the interior of the island, most significantly in the Sprengisandur and Þórisvatn area to the west and northwest of Vatnajökull. Closer to the coast, seasonal variability is well-represented by analyses. Also, on sub-monthly time-scales, analysed variability of surface air temperature within the interior is significantly too low compared with observations.

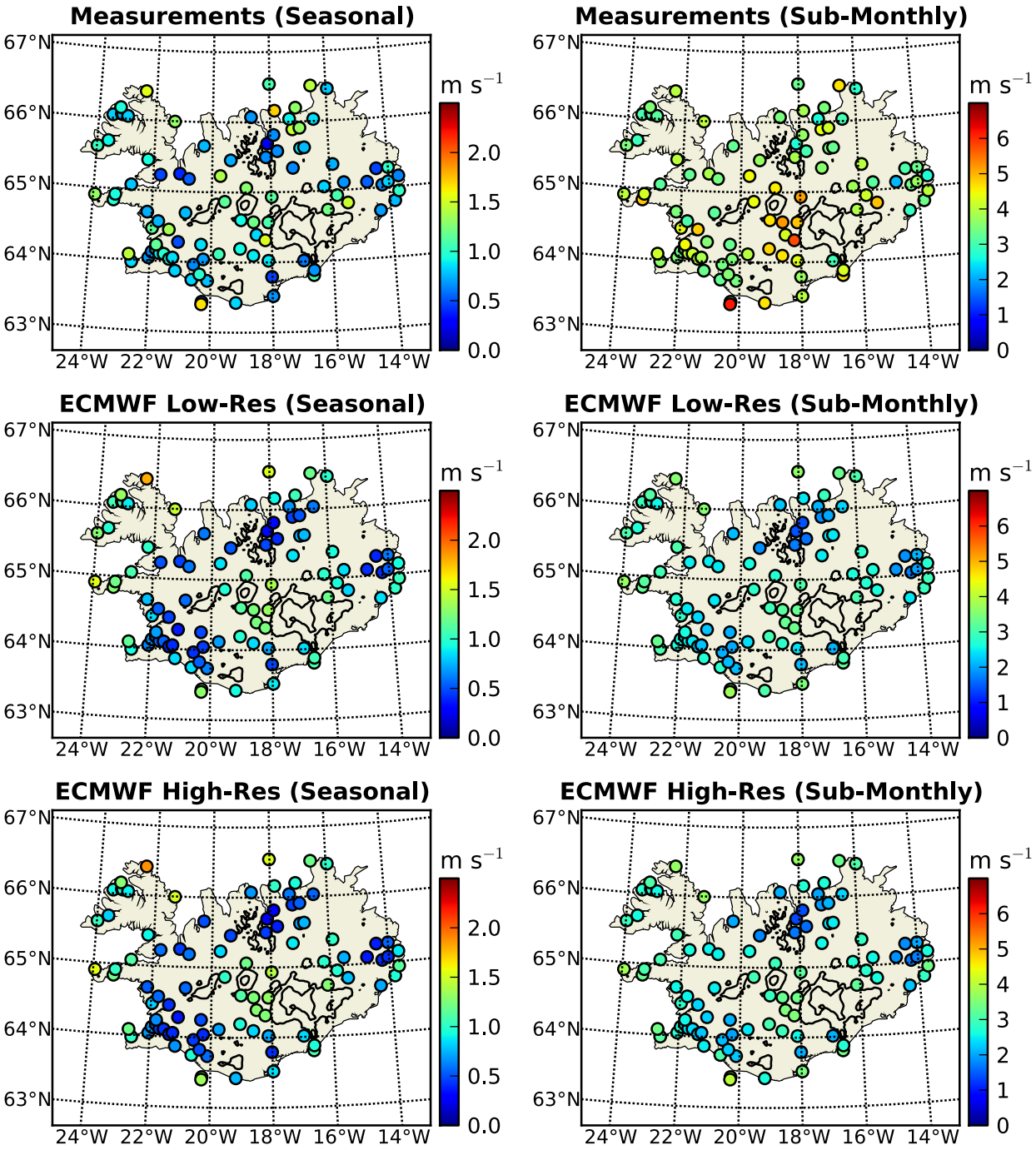


*Figure 24. Temporal variability on seasonal and sub-monthly time-scales (see Section 6) of surface wind speed based on 6-hourly local observational time-series and linearly interpolated operational analyses.*

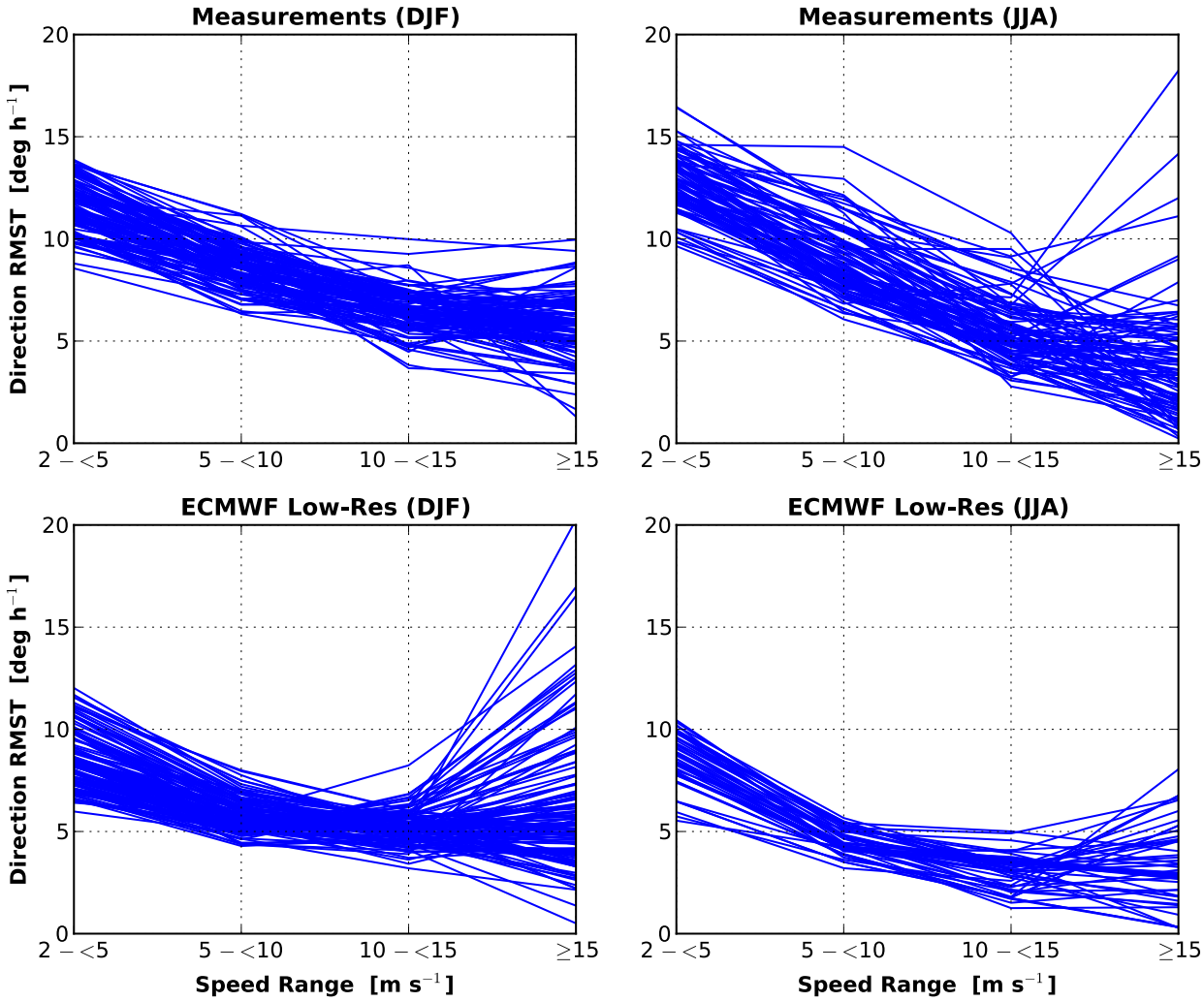


*Figure 25. Root mean square tendency (RMST) of surface wind direction as a function of wind speed in winter (DJF) and summer (JJA) for hourly local and regionally averaged observational time-series.*

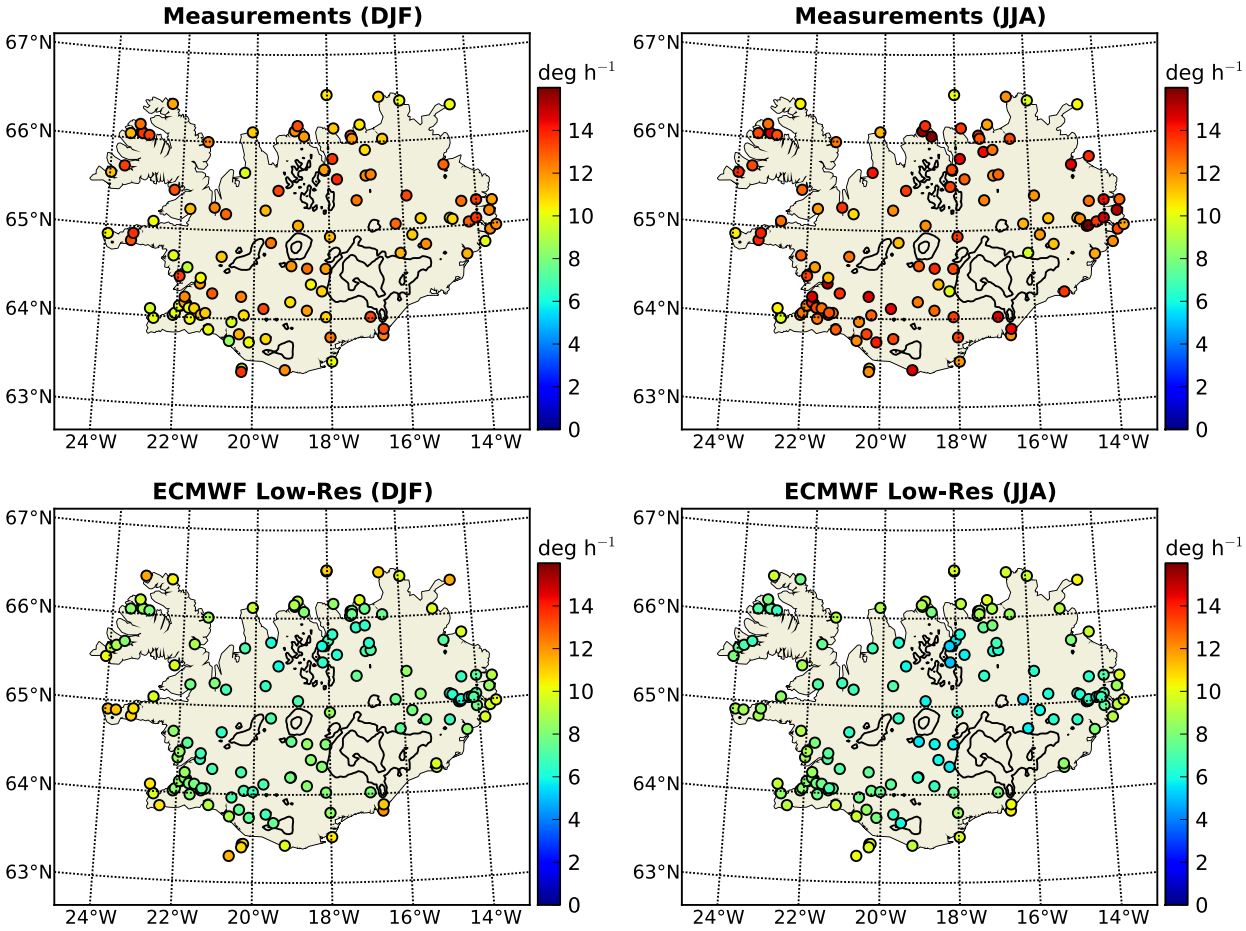


*Figure 26. Root mean square tendency of surface wind direction in winter (DJF) and summer (JJA) at station locations for hourly local and regionally averaged observational time-series, taking into account low surface wind speeds ($2 \leq$ speed $< 5$ m s$^{-1}$).*

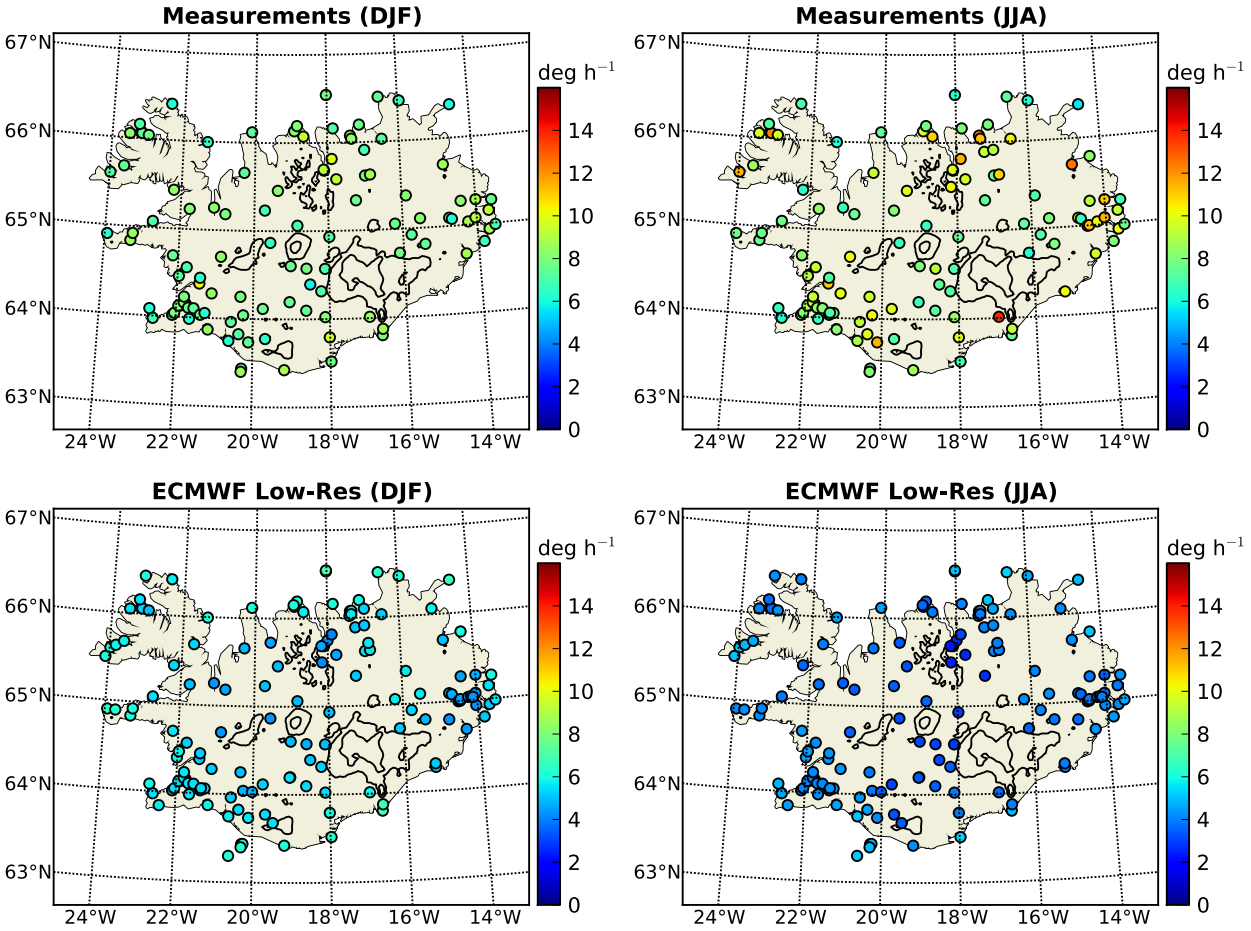


*Figure 27. Root mean square tendency of surface wind direction in winter (DJF) and summer (JJA) at station locations for hourly local and regionally averaged observational time-series, taking into account intermediate to high surface wind speeds (*speed $\geq 5$ m s$^{-1}$*).*

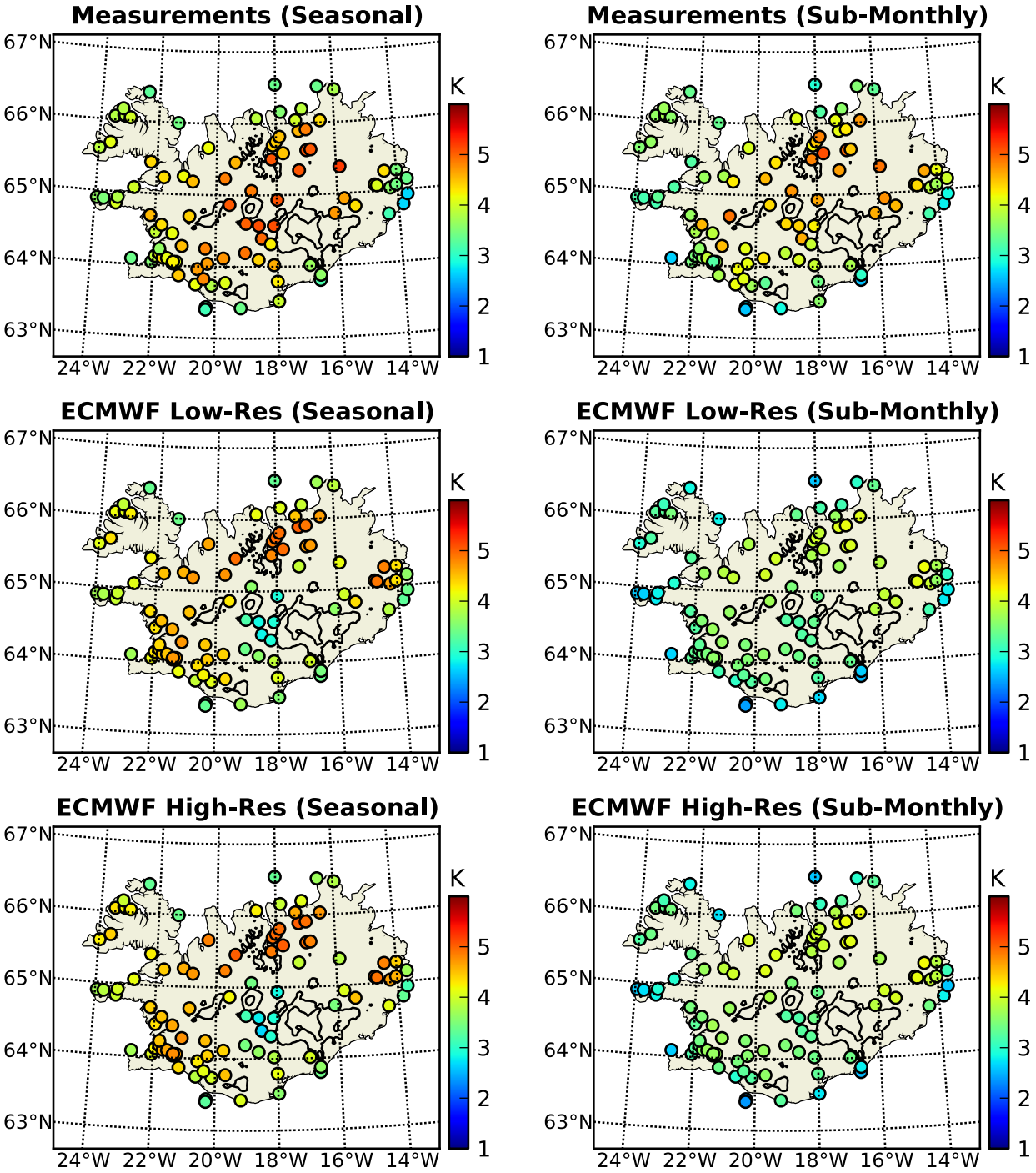


*Figure 28. Temporal variability on seasonal and sub-monthly time-scales (see Section 6) of surface air temperature based on 6-hourly local observational time-series and linearly interpolated operational analyses.*

# 7 Summary

In this report, an analysis is presented of the station record for surface wind and temperature over Iceland during the 1 Nov 2005 to 31 Oct 2009 period, considering all stations with at least 75% of valid data. These results are compared with operational surface analyses from the European Centre for Medium-Range Weather Forecasts. Different selection methods for values corresponding to station locations from the gridded analysis fields were discussed. The relative performance of different methods varies along the coast. However, it was argued that overall the best results are obtained by linear interpolation.

*Surface Wind Conditions*

No significant differences are found between seasonal averages based on either hourly or 6-hourly time-series.

Generally, winds are weaker in summer than in winter, consistent with weaker pressure gradients over the island. In winter and summer, the highest regional wind speeds are found in the interior. In winter, intermediate and high wind speeds at low elevations also exist along the north and southwest coast. Regionally the weakest surface winds in winter occur in the Westfjords and the eastern part of the island. In summer, the weakest regional winds are found in the Westfjords. Especially in the Westfjords, this is most likely due to the strong terrain sheltering at low-lying observation sites. Based on the large-scale pressure gradients over that region, winds over higher terrain are likely to be intense.

For weak winds, the influence of temperature gradients is clearly noticeable at nearly all locations. Especially during winter, prevailing surface winds flow from low to high temperatures, downslope in the interior of the island, and off-shore along the coast. In summer, land – sea temperature gradients result in prevailing on-shore winds in most places. Exceptions are found at outlying locations in the north, where east-northeasterly surface winds are affected by large-scale pressure gradients, as well as in the southwest region, where summertime temperature gradients are weak.

For intermediate to strong surface winds in both seasons, easterly and southeasterly directions prevail near the coast in the western part of the island, where large scale geostrophic winds combine with local temperature gradients. Inconsistency between large-scale and local forcing in the east results in weaker average wind vectors.

On monthly to annual time-scales, no significant differences exist between variability of hourly and 6-hourly time-series. On a seasonal time-scale, there is no consistent spatial pattern in temporal variability. On shorter time-scales up to one month, with the exception of a few high outliers at the coast, temporal variability generally decreases from the centre of the island outwards.

Root mean square tendency of surface wind direction decreases with wind speed. It has the lowest regional values over Reykjanes, and the highest regional values in the east, the north, and over the Westfjords. Wind direction variability generally increases in summer, as thermal wind systems become more prevalent.

The increase in wind speed with terrain elevation, seen in observations, is underestimated in operational analyses, since the model terrain is considerably too low. Additionally, there is a decrease in analysed wind speed in regions with rugged terrain. Consequently, analysed wind speeds in the interior of the island are almost exclusively too low. Too high values are found primarily on Snæfellsnes, and to a lesser extent at some locations along the north coast. Aside from these differences in absolute values, the timing of monthly minima and maxima throughout the year is well represented in operational analyses.

In winter, the prevailing off-shore flow is also well represented in analyses. However, in summer, winds along the north coast have a too strong northerly component, while there are too strong easterly average wind vectors in the Þórisvatn area.

*Surface Air Temperature*

There is a well-defined decrease in seasonal averages of surface air temperature with local terrain elevation. Therefore, in winter and summer, the lowest temperatures exist in the interior of the island. In winter, temperatures along the coast vary little, with only slightly higher values in the south. In summer, the highest temperatures at low elevations are found in the southwest.

In winter, the coldest temperatures over land are situated further northeast with on-shore than with off-shore winds. Also, the temperatures in the southwest are significantly warmer with on-shore winds. These changes are well represented in the operational analyses. This increase in the northeast to southwest temperature gradient across the island with on-shore winds is consistent with differential temperature advection associated with the north to south gradient in air and sea surface temperatures. In summer, low-elevation measured and analysed surface air temperatures near the coast are very similar to the surrounding sea surface temperatures. Consequently, there is no significant impact on average land-based temperatures from winds with either on- or off-shore directions.

The seasonal cycle of surface air temperature is largest in the centre of the island. Variability on shorter time-scales of up to one month is highest in the region of relatively flat terrain between Mývatn and the northern slopes of Vatnajökull.

Surface air temperatures in operational analyses in the interior of the island are consistently too high compared with measurements in winter, and too low in summer. The seasonal cycle in surface air temperature in the interior of the island is therefore significantly underestimated, especially in the Sprengisandur and Þórisvatn area to the west and northwest of Vatnajökull. Closer to the coast, seasonal variability is well-represented by the operational analyses. On sub-monthly time-scales, analysed variability of surface air temperature within the high interior is slightly larger than for seasonal time-scales, but remains too low compared with observations.

# References


Andersson, E. and Thépaut, J. N. (2008). ECMWF's 4D-Var data assimilation system – the genesis and ten years in operations. *ECMWF Newsletter*, 115:8–12.

Björnsson, H., Jónsson, T., Gylfadóttir, S. S., and Ólason, E. Ó. (2007). Mapping the annual cycle of temperature in Iceland. *Meteorol. Z.*, 16(1):45–56.

Blöndal, J., Birgisson, T., Björnsson, H., Jónasson, K., and Petersen, G. N. (2011). Vindhraðamælingar og sambreytni vinds. Report VÍ 2011-014, Icelandic Meteorological Office, Reykjavik, Iceland.

Courtier, P. (1997). Dual formulation of four-dimensional variational assimilation. *Quart. J. Roy. Meteor. Soc.*, 123:2449–2461.

Crochet, P. and Jóhannesson, T. (2011). A data set of gridded daily temperature in Iceland, 1949-2010. *Jökull*, 61:1–18.

Einarsson, M. Á. (1984). Chapter 7: Climate of iceland. In van Loon, H., editor, *Climates of the Oceans*, volume 15 of *World Survey of Climatology*, pages 673–697, Amsterdam, Netherlands. Elsevier.

Gylfadóttir, S. S. (2003). Spatial interpolation of Icelandic monthly mean temperature data. Report VÍ-ÚR06 03006, Icelandic Meteorological Office, Reykjavik, Iceland.

Nawri, N., Björnsson, H., Jónasson, K., and Petersen, G. N. (2012a). Empirical terrain models for surface wind and air temperature over Iceland. Report VÍ 2012-009, Icelandic Meteorological Office, Reykjavik, Iceland.

Nawri, N., Björnsson, H., Jónasson, K., and Petersen, G. N. (2012b). Evaluation of WRF mesoscale model simulations of surface wind over Iceland. Report VÍ 2012-010, Icelandic Meteorological Office, Reykjavik, Iceland.

Nawri, N., Björnsson, H., Jónasson, K., and Petersen, G. N. (2012c). Statistical correction of WRF mesoscale model simulations of surface wind over Iceland based on station data. Report VÍ 2012-011, Icelandic Meteorological Office, Reykjavik, Iceland.

Skamarock, W. C., Klemp, J. B., Dudhia, J., Gill, D. O., Barker, D. M., Duda, M. G., Huang, X.-Y., Wang, W., and Powers, J. G. (2008). A description of the Advanced Research WRF Version 3. NCAR Technical Note NCAR/TN-475+STR, National Center for Atmospheric Research, Boulder, Colorado, USA.

WMO (2008). *Guide to Meteorological Instruments and Methods of Observation, WMO-No. 8, 7th Edition*. World Meteorological Organization, Geneva, Switzerland.

# A Surface Weather Stations

Lists of all surface weather stations used in this study, ordered by name or identification number.

*Table 1. Surface weather stations ordered by name.*

| Location | Station ID | Longitude [°E] | Latitude [°N] |
|---|---|---|---|
| Akureyri - Krossanesbraut | 3471 | -18.111 | 65.696 |
| Akureyri lögreglustöð | 3470 | -18.100 | 65.686 |
| Árnes | 6420 | -20.252 | 64.041 |
| Ásbyrgi | 4614 | -16.483 | 66.030 |
| Ásgarður sjálfvirk stöð | 2175 | -21.754 | 65.230 |
| Básar á Goðalandi | 6237 | -19.481 | 63.679 |
| Bíldudalur | 2428 | -23.612 | 65.679 |
| Bjarnarey | 4472 | -14.317 | 65.783 |
| Bjarnarflag | 4303 | -16.837 | 65.630 |
| Bláfeldur sjálfvirk stöð | 1936 | -23.301 | 64.839 |
| Bláfjallaskáli | 1487 | -21.650 | 63.983 |
| Blönduós | 3317 | -20.293 | 65.658 |
| Bolungarvík sjálfvirk stöð | 2738 | -23.254 | 66.161 |
| Botnsheiði | 1689 | -21.403 | 64.453 |
| Brú á Jökuldal | 5940 | -15.530 | 65.109 |
| Brúarjökull B10 | 5932 | -16.112 | 64.728 |
| Brúðardalur | 5968 | -14.511 | 64.996 |
| Búrfell | 6430 | -19.745 | 64.117 |
| Dalatangi sjálfvirk stöð | 4193 | -13.575 | 65.268 |
| Egilsstaðaflugvöllur sjálfvirk stöð | 4271 | -14.405 | 65.276 |
| Eskifjörður | 5981 | -14.037 | 65.076 |
| Eyjabakkar | 5943 | -15.423 | 64.815 |
| Eyrarbakki sjálfvirk stöð | 1395 | -21.160 | 63.869 |
| Fagurhólsmýri sjálfvirk stöð | 5309 | -16.636 | 63.874 |
| Fáskrúðsfjörður Ljósaland | 5982 | -14.041 | 64.937 |
| Fíflholt á Mýrum | 1868 | -22.147 | 64.694 |
| Flatey á Skjálfanda | 3779 | -17.841 | 66.163 |
| Flateyri | 2631 | -23.510 | 66.050 |
| Fontur | 4867 | -14.533 | 66.378 |
| Garðskagaviti | 1453 | -22.689 | 64.082 |

*Table 1. Continued.*

| Location | Station ID | Longitude [°E] | Latitude [°N] |
|---|---|---|---|
| Geldinganes | 1480 | -21.804 | 64.168 |
| Gjögurflugvöllur | 2692 | -21.330 | 65.995 |
| Grindavík | 1361 | -22.417 | 63.844 |
| Grímsey | 3976 | -18.017 | 66.544 |
| Grundarfjörður | 1938 | -23.251 | 64.921 |
| Gufuskálar | 1919 | -23.933 | 64.900 |
| Hafnarmelar | 1673 | -21.963 | 64.465 |
| Hallormsstaðaháls | 5960 | -14.675 | 65.080 |
| Hallormsstaður | 4060 | -14.745 | 65.094 |
| Hallsteinsdalsvarp | 5970 | -14.453 | 65.018 |
| Haugur sjálfvirk stöð | 3103 | -20.785 | 65.184 |
| Hágöngur | 6776 | -18.111 | 64.571 |
| Hella sjálfvirk stöð | 6315 | -20.365 | 63.826 |
| Hellisskarð | 1490 | -21.367 | 64.033 |
| Hjarðarland sjálfvirk stöð | 6515 | -20.331 | 64.251 |
| Hornbjargsviti | 2862 | -22.379 | 66.411 |
| Hólmavík | 2481 | -21.681 | 65.687 |
| Hólmsheiði | 1481 | -21.686 | 64.109 |
| Húsafell | 6802 | -20.869 | 64.699 |
| Húsavík | 3696 | -17.328 | 66.042 |
| Húsavík Héðinshöfði | 3695 | -17.322 | 66.080 |
| Hvanneyri | 1779 | -21.767 | 64.567 |
| Hvassahraun | 1370 | -22.092 | 64.020 |
| Hveravellir sjálfvirk stöð | 6935 | -19.562 | 64.867 |
| Höfn í Hornafirði sjálfvirk stöð | 5544 | -15.214 | 64.269 |
| Ingólfshöfði | 5210 | -16.651 | 63.803 |
| Ísafjörður sjálfvirk stöð | 2642 | -23.170 | 66.060 |
| Jökulheimar | 6670 | -18.217 | 64.317 |
| Kambanes | 5885 | -13.842 | 64.801 |
| Kálfhóll | 6310 | -20.567 | 63.963 |
| Kárahnjúkar | 5933 | -15.777 | 64.928 |
| Keflavíkurflugvöllur sjálfvirk stöð | 1350 | -22.589 | 63.974 |
| Kirkjubæjarklaustur - Stjórnarsandur | 6272 | -18.012 | 63.793 |
| Kolka | 3225 | -19.717 | 65.233 |

*Table 1. Continued.*

| Location | Station ID | Longitude [°E] | Latitude [°N] |
|---|---|---|---|
| Kollaleira sjálfvirk stöð | 5975 | -14.240 | 65.037 |
| Korpa | 1479 | -21.751 | 64.151 |
| Krókóttuvötn Reykjahlíðarheiði | 4404 | -16.879 | 65.710 |
| Lambavatn | 2315 | -24.093 | 65.492 |
| Laufbali | 6472 | -18.120 | 64.024 |
| Lónakvísl | 6459 | -18.614 | 64.098 |
| Mánárbakki sjálfvirk stöð | 3797 | -17.103 | 66.199 |
| Miðdalsheiði | 1483 | -21.545 | 64.104 |
| Miðfjarðarnes | 4652 | -15.080 | 66.067 |
| Mývatn | 4300 | -16.977 | 65.620 |
| Möðrudalur sjálfvirk stöð | 4830 | -15.883 | 65.375 |
| Mörk á Landi | 6424 | -20.019 | 64.029 |
| Nautabú sjálfvirk stöð | 3242 | -19.369 | 65.458 |
| Neskaupstaður sjálfvirk stöð | 5990 | -13.669 | 65.150 |
| Ólafsfjörður | 3658 | -18.666 | 66.074 |
| Ólafsvík | 1924 | -23.714 | 64.895 |
| Patreksfjörður | 2319 | -23.975 | 65.595 |
| Rauðinúpur | 4912 | -16.544 | 66.508 |
| Raufarhöfn sjálfvirk stöð | 4828 | -15.953 | 66.456 |
| Reykhólar sjálfvirk stöð | 2266 | -22.206 | 65.438 |
| Reykir í Fnjóskadal | 3380 | -17.767 | 65.585 |
| Reykir í Hrútafirði sjálfvirk stöð | 2197 | -21.098 | 65.254 |
| Reykjavík sjálfvirk stöð | 1475 | -21.902 | 64.128 |
| Reykjavíkurflugvöllur | 1477 | -21.941 | 64.128 |
| Sandbúðir | 6975 | -17.983 | 64.933 |
| Sauðárkrókur flugvöllur | 3433 | -19.574 | 65.726 |
| Sámsstaðir | 6222 | -20.109 | 63.735 |
| Sáta | 3054 | -18.838 | 65.063 |
| Seley | 5993 | -13.517 | 64.983 |
| Seljalandsdalur - skíðaskáli | 2641 | -23.210 | 66.069 |
| Setur | 6748 | -19.019 | 64.604 |
| Seyðisfjörður | 4180 | -14.000 | 65.281 |
| Siglufjörður | 3752 | -18.919 | 66.135 |
| Siglunes | 3754 | -18.843 | 66.194 |

*Table 1. Continued.*

| Location | Station ID | Longitude [°E] | Latitude [°N] |
|---|---|---|---|
| Skaftafell | 6499 | -16.967 | 64.016 |
| Skagatá | 3720 | -20.099 | 66.119 |
| Skarðsfjöruviti | 6176 | -17.979 | 63.518 |
| Skarðsmýrarfjall | 1496 | -21.347 | 64.057 |
| Skjaldþingsstaðir sjálfvirk stöð | 4455 | -14.821 | 65.704 |
| Skrauthólar | 1578 | -21.805 | 64.232 |
| Sóleyjarflatamelar | 3595 | -17.227 | 65.891 |
| Stórhöfði sjálfvirk stöð | 6017 | -20.288 | 63.400 |
| Straumnesviti | 2941 | -23.133 | 66.433 |
| Straumsvík | 1473 | -22.040 | 64.044 |
| Stykkishólmur sjálfvirk stöð | 2050 | -22.732 | 65.072 |
| Surtsey | 6012 | -20.599 | 63.299 |
| Súðavík | 2646 | -22.986 | 66.043 |
| Svartárkot sjálfvirk stöð | 3292 | -17.243 | 65.342 |
| Tálknafjörður | 2323 | -23.830 | 65.628 |
| Teigarhorn sjálfvirk stöð | 5872 | -14.344 | 64.676 |
| Tindfjöll | 6235 | -19.677 | 63.776 |
| Torfur sjálfvirk stöð | 3371 | -18.162 | 65.501 |
| Upptyppingar | 4019 | -16.210 | 65.061 |
| Vaðlaheiði | 3474 | -18.001 | 65.749 |
| Vatnsfell | 6546 | -19.047 | 64.196 |
| Vatnsskarðshólar sjálfvirk stöð | 6045 | -19.183 | 63.424 |
| Vattarnes | 5988 | -13.685 | 64.937 |
| Veiðivatnahraun | 6657 | -18.505 | 64.395 |
| Vestmannaeyjabær | 6015 | -20.276 | 63.436 |
| Végeirsstaðir í Fnjóskadal | 3477 | -17.886 | 65.817 |
| Þeistareykir | 4500 | -16.976 | 65.911 |
| Þingvellir | 1596 | -21.088 | 64.280 |
| Þórdalsheiði | 5969 | -14.462 | 65.001 |
| Þúfuver | 6760 | -18.601 | 64.575 |
| Þykkvibær | 6208 | -20.618 | 63.748 |
| Þyrill | 1685 | -21.417 | 64.388 |
| Ölkelduháls | 1493 | -21.253 | 64.055 |

*Table 2. Surface weather stations ordered by identification number.*

| Location | Station ID | Longitude [°E] | Latitude [°N] |
|---|---|---|---|
| Keflavíkurflugvöllur sjálfvirk stöð | 1350 | -22.589 | 63.974 |
| Grindavík | 1361 | -22.417 | 63.844 |
| Hvassahraun | 1370 | -22.092 | 64.020 |
| Eyrarbakki sjálfvirk stöð | 1395 | -21.160 | 63.869 |
| Garðskagaviti | 1453 | -22.689 | 64.082 |
| Straumsvík | 1473 | -22.040 | 64.044 |
| Reykjavík sjálfvirk stöð | 1475 | -21.902 | 64.128 |
| Reykjavíkurflugvöllur | 1477 | -21.941 | 64.128 |
| Korpa | 1479 | -21.751 | 64.151 |
| Geldinganes | 1480 | -21.804 | 64.168 |
| Hólmsheiði | 1481 | -21.686 | 64.109 |
| Miðdalsheiði | 1483 | -21.545 | 64.104 |
| Bláfjallaskáli | 1487 | -21.650 | 63.983 |
| Hellisskarð | 1490 | -21.367 | 64.033 |
| Ölkelduháls | 1493 | -21.253 | 64.055 |
| Skarðsmýrarfjall | 1496 | -21.347 | 64.057 |
| Skrauthólar | 1578 | -21.805 | 64.232 |
| Þingvellir | 1596 | -21.088 | 64.280 |
| Hafnarmelar | 1673 | -21.963 | 64.465 |
| Þyrill | 1685 | -21.417 | 64.388 |
| Botnsheiði | 1689 | -21.403 | 64.453 |
| Hvanneyri | 1779 | -21.767 | 64.567 |
| Fíflholt á Mýrum | 1868 | -22.147 | 64.694 |
| Gufuskálar | 1919 | -23.933 | 64.900 |
| Ólafsvík | 1924 | -23.714 | 64.895 |
| Bláfeldur sjálfvirk stöð | 1936 | -23.301 | 64.839 |
| Grundarfjörður | 1938 | -23.251 | 64.921 |
| Stykkishólmur sjálfvirk stöð | 2050 | -22.732 | 65.072 |
| Ásgarður sjálfvirk stöð | 2175 | -21.754 | 65.230 |
| Reykir í Hrútafirði sjálfvirk stöð | 2197 | -21.098 | 65.254 |
| Reykhólar sjálfvirk stöð | 2266 | -22.206 | 65.438 |
| Lambavatn | 2315 | -24.093 | 65.492 |
| Patreksfjörður | 2319 | -23.975 | 65.595 |

*Table 2. Continued.*

| Location | Station ID | Longitude [°E] | Latitude [°N] |
|---|---|---|---|
| Tálknafjörður | 2323 | -23.830 | 65.628 |
| Bíldudalur | 2428 | -23.612 | 65.679 |
| Hólmavík | 2481 | -21.681 | 65.687 |
| Flateyri | 2631 | -23.510 | 66.050 |
| Seljalandsdalur - skíðaskáli | 2641 | -23.210 | 66.069 |
| Ísafjörður sjálfvirk stöð | 2642 | -23.170 | 66.060 |
| Súðavík | 2646 | -22.986 | 66.043 |
| Gjögurflugvöllur | 2692 | -21.330 | 65.995 |
| Bolungarvík sjálfvirk stöð | 2738 | -23.254 | 66.161 |
| Hornbjargsviti | 2862 | -22.379 | 66.411 |
| Straumnesviti | 2941 | -23.133 | 66.433 |
| Sáta | 3054 | -18.838 | 65.063 |
| Haugur sjálfvirk stöð | 3103 | -20.785 | 65.184 |
| Kolka | 3225 | -19.717 | 65.233 |
| Nautabú sjálfvirk stöð | 3242 | -19.369 | 65.458 |
| Svartárkot sjálfvirk stöð | 3292 | -17.243 | 65.342 |
| Blönduós | 3317 | -20.293 | 65.658 |
| Torfur sjálfvirk stöð | 3371 | -18.162 | 65.501 |
| Reykir í Fnjóskadal | 3380 | -17.767 | 65.585 |
| Sauðárkrókur flugvöllur | 3433 | -19.574 | 65.726 |
| Akureyri lögreglustöð | 3470 | -18.100 | 65.686 |
| Akureyri - Krossanesbraut | 3471 | -18.111 | 65.696 |
| Vaðlaheiði | 3474 | -18.001 | 65.749 |
| Végeirsstaðir í Fnjóskadal | 3477 | -17.886 | 65.817 |
| Sóleyjarflatamelar | 3595 | -17.227 | 65.891 |
| Ólafsfjörður | 3658 | -18.666 | 66.074 |
| Húsavík Héðinshöfði | 3695 | -17.322 | 66.080 |
| Húsavík | 3696 | -17.328 | 66.042 |
| Skagatá | 3720 | -20.099 | 66.119 |
| Siglufjörður | 3752 | -18.919 | 66.135 |
| Siglunes | 3754 | -18.843 | 66.194 |
| Flatey á Skjálfanda | 3779 | -17.841 | 66.163 |
| Mánárbakki sjálfvirk stöð | 3797 | -17.103 | 66.199 |

*Table 2. Continued.*

| Location | Station ID | Longitude [°E] | Latitude [°N] |
|---|---|---|---|
| Grímsey | 3976 | -18.017 | 66.544 |
| Upptyppingar | 4019 | -16.210 | 65.061 |
| Hallormsstaður | 4060 | -14.745 | 65.094 |
| Seyðisfjörður | 4180 | -14.000 | 65.281 |
| Dalatangi sjálfvirk stöð | 4193 | -13.575 | 65.268 |
| Egilsstaðaflugvöllur sjálfvirk stöð | 4271 | -14.405 | 65.276 |
| Mývatn | 4300 | -16.977 | 65.620 |
| Bjarnarflag | 4303 | -16.837 | 65.630 |
| Krókóttuvötn Reykjahlíðarheiði | 4404 | -16.879 | 65.710 |
| Skjaldþingsstaðir sjálfvirk stöð | 4455 | -14.821 | 65.704 |
| Bjarnarey | 4472 | -14.317 | 65.783 |
| Þeistareykir | 4500 | -16.976 | 65.911 |
| Ásbyrgi | 4614 | -16.483 | 66.030 |
| Miðfjarðarnes | 4652 | -15.080 | 66.067 |
| Raufarhöfn sjálfvirk stöð | 4828 | -15.953 | 66.456 |
| Möðrudalur sjálfvirk stöð | 4830 | -15.883 | 65.375 |
| Fontur | 4867 | -14.533 | 66.378 |
| Rauðinúpur | 4912 | -16.544 | 66.508 |
| Ingólfshöfði | 5210 | -16.651 | 63.803 |
| Fagurhólsmýri sjálfvirk stöð | 5309 | -16.636 | 63.874 |
| Höfn í Hornafirði sjálfvirk stöð | 5544 | -15.214 | 64.269 |
| Teigarhorn sjálfvirk stöð | 5872 | -14.344 | 64.676 |
| Kambanes | 5885 | -13.842 | 64.801 |
| Brúarjökull B10 | 5932 | -16.112 | 64.728 |
| Kárahnjúkar | 5933 | -15.777 | 64.928 |
| Brú á Jökuldal | 5940 | -15.530 | 65.109 |
| Eyjabakkar | 5943 | -15.423 | 64.815 |
| Hallormsstaðaháls | 5960 | -14.675 | 65.080 |
| Brúðardalur | 5968 | -14.511 | 64.996 |
| Þórdalsheiði | 5969 | -14.462 | 65.001 |
| Hallsteinsdalsvarp | 5970 | -14.453 | 65.018 |
| Kollaleira sjálfvirk stöð | 5975 | -14.240 | 65.037 |
| Eskifjörður | 5981 | -14.037 | 65.076 |

*Table 2. Continued.*

| Location | Station ID | Longitude [°E] | Latitude [°N] |
|---|---|---|---|
| Fáskrúðsfjörður Ljósaland | 5982 | -14.041 | 64.937 |
| Vattarnes | 5988 | -13.685 | 64.937 |
| Neskaupstaður sjálfvirk stöð | 5990 | -13.669 | 65.150 |
| Seley | 5993 | -13.517 | 64.983 |
| Surtsey | 6012 | -20.599 | 63.299 |
| Vestmannaeyjabær | 6015 | -20.276 | 63.436 |
| Stórhöfði sjálfvirk stöð | 6017 | -20.288 | 63.400 |
| Vatnsskarðshólar sjálfvirk stöð | 6045 | -19.183 | 63.424 |
| Skarðsfjöruviti | 6176 | -17.979 | 63.518 |
| Þykkvibær | 6208 | -20.618 | 63.748 |
| Sámsstaðir | 6222 | -20.109 | 63.735 |
| Tindfjöll | 6235 | -19.677 | 63.776 |
| Básar á Goðalandi | 6237 | -19.481 | 63.679 |
| Kirkjubæjarklaustur - Stjórnarsandur | 6272 | -18.012 | 63.793 |
| Kálfhóll | 6310 | -20.567 | 63.963 |
| Hella sjálfvirk stöð | 6315 | -20.365 | 63.826 |
| Árnes | 6420 | -20.252 | 64.041 |
| Mörk á Landi | 6424 | -20.019 | 64.029 |
| Búrfell | 6430 | -19.745 | 64.117 |
| Lónakvísl | 6459 | -18.614 | 64.098 |
| Laufbali | 6472 | -18.120 | 64.024 |
| Skaftafell | 6499 | -16.967 | 64.016 |
| Hjarðarland sjálfvirk stöð | 6515 | -20.331 | 64.251 |
| Vatnsfell | 6546 | -19.047 | 64.196 |
| Veiðivatnahraun | 6657 | -18.505 | 64.395 |
| Jökulheimar | 6670 | -18.217 | 64.317 |
| Setur | 6748 | -19.019 | 64.604 |
| Þúfuver | 6760 | -18.601 | 64.575 |
| Hágöngur | 6776 | -18.111 | 64.571 |
| Húsafell | 6802 | -20.869 | 64.699 |
| Hveravellir sjálfvirk stöð | 6935 | -19.562 | 64.867 |
| Sandbúðir | 6975 | -17.983 | 64.933 |